



MONASH University

**Interactive and dynamic visualization
of high-dimensional data via animated
linear projections, their efficacy, and
their application to local explanations
of non-linear models**

Nicholas Spyris

B.Sc. Statistics, Iowa State University

A thesis submitted for the degree of Doctor of Philosophy at

Monash University in January 2022

Department of Human-Centred Computing

January 2022

Contents

Copyright notice	v
Abstract	vii
Declaration	1
Acknowledgments	5
Preface	7
1 Introduction	9
1.1 Research questions	10
1.2 Methodology	11
1.3 Contributions	12
1.4 Background	13
1.5 Thesis structure	20
2 spinifex: an R package for creating user-controlled animated linear projections	21
2.1 Introduction	22
2.2 Algorithm	23
2.3 Package structure	29
2.4 Use cases	31
2.5 Discussion	35
2.6 Acknowledgments	36
3 The benefit of user-controlled radial tour for understanding variable contributions to structure in linear projections	37
3.1 Introduction	38
3.2 Background	39
3.3 User study	44
3.4 Results	53
3.5 Conclusion	58
3.6 Accompanying tool: radial tour application	58
3.7 Acknowledgments	59
3.8 References	59
3.9 Appendix	59

4 Scrutinizing the linear variable importance of local explanations of non-linear models with animated linear projections	67
4.1 Introduction	68
4.2 Local explanation statistics	70
4.3 Tours and the radial tour	73
4.4 Cheem viewer	74
4.5 Case studies	80
4.6 Discussion	86
4.7 Acknowledgments	87
4.8 References	87
5 Conclusion	89
5.1 Software development	89
5.2 Further extensions	90
5.3 Other contributions	91
Bibliography	93

Copyright notice

© Nicholas Spyrisson (2022).

I certify that I have made all reasonable efforts to secure copyright permissions for third-party content included in this thesis and have not knowingly added copyright content to my work without the owner's permission.

Abstract

Visualizing data space is crucial to exploratory data analysis, checking model assumptions, and validating model performance. Yet visualization quickly becomes difficult as the dimensionality of the data or features increases. Traditionally, static, low-dimensional linear embeddings are used to mitigate this complexity. Such embedded space is a lossy approximation of the full space. However, viewing many embeddings with interactive supporting views improves the information conveyed. Data visualization *tours* are a class of dynamic linear projections that animate many linear projections over small changes to the projection basis.

Tours are categorized by the path of their bases. *Manual tours* allow for User-Controlled Steering (UCS) of bases path, where the contributions of individual variables can be controlled. I create a free, open-source **R** package, **spinifex**, that facilitates creating such tours. These manipulations of the variables can be precomputed or made in real-time. Display composition and exportable formats are interoperable with the existing package **tourr** and can be rendered with recent graphics interfaces **plotly** and **ganimate**. The former offers interactive use with HTML widgets, while the latter can render to static formats such as .gif or .mp4 files. An interactive application is included to illustrate the use of the manual tour.

Theoretically, the UCS of the manual tour should enable an analyst to better explore the variable attribution to the structure identified in an embedding. I find strong evidence to support that radial tour leads to a significant and large increase in accuracy as compared with Principal Component Analysis (PCA) and an alternative tour variant, the grand tour. I conduct a within-participant, crowd-sourced user study comparing these visualization

methods. Each of the $n = 108$ participants performs two trials with each visual for 648 total trials. The task is a supervised classification problem asking participants which variables attribute to the separation of 2 clusters.

Modern modeling techniques are sometimes referred to as black-box models due to the uninterpretable nature of model terms which are often many and non-linear. Recent research in Explainable Artificial Intelligence (XAI) tries to bring interpretability to these models through *local explanations*. Local explanations are a class of techniques that approximate the linear-variable importance at one point in the data. I build an **cheem**, an **R** package to streamline model and local explanation preprocessing, and two novel visuals. First the global view pits the data- and explanation-spaces side-by-side with a residual plot. Interactive features such as linked bushing and tooltips aid in identifying observations to compare. The local explanation from the selected observation becomes a basis used in creating the radial tour. This allows an analyst to evaluate the explanation and explore the sensitivity of the explanation to changes in the variable contribution.

Declaration

I hereby declare that this thesis contains no material which has been accepted for the award of any other degree or diploma at any university or equivalent institution and that, to the best of my knowledge and belief, this thesis contains no material previously published or written by another person, except where due reference is made in the text of the thesis.

Three publications are included in this thesis, one of which has been accepted for publication in *The R Journal* (Spyrison and Cook, 2020). The user study described in Chapter 3 will shortly be submitted to the *Journal of Data Science, Statistics, and Visualisation*. The research covered in Chapter 4 will shortly be submitted to *IEEE Transactions on Knowledge and Data Engineering*.

All of the papers in the thesis were conceptualized, developed, and written by myself, the student, while working in the Department of Human-Centered Computing under the supervision of professor Kimbal Marriott and professor Dianne Cook. When co-authors are listed, it indicates that the work was produced through active collaboration between researchers and that their contributions to team-based research have been recognized. The following table details the work, including my and my fellow co-authors' contributions.

I have renumbered and updated sections of submitted or published papers to generate a consistent presentation within the thesis.

Student name: Nicholas Spyrison

Student signature:

CONTENTS

Thesis Chapter	Publication Title	Status (published, in press, accepted or re-turned for revision)	Nature and % of student contribution	Co-author name(s) Nature and % of Co-author's contribution	Co-author(s), Monash student Y/N
3	spinifex: an R package for creating user-controlled animated linear projections	75%. Concept, development, writing first draft and software development	(1) Dianne Cook, concept, methodology, writing 25%	N	
4	The benefit of user-controlled radial tour for understanding variable contributions to structure in linear projections	To be submitted	80%. Concept, development, writing first draft, application, and conducting user study	(1) Dianne Cook, Concept, methodology, editing 12% (2) Kimbal Marriott, concept, methodology, editing 8%	N
5	Interrogating the linear variable importance of local explanations of non-linear models with animated linear projections	To be submitted	85%. Concept, development, writing first draft and software development	(1) Dianne Cook, methodology, editing 10% (2) Kimbal Marriott, methodology, editing 5%	N

Nicholas Spenjers

Date: 2021-12-12

The undersigned hereby certify that the above declaration correctly reflects the nature and extent of the student's co-authors' contribution to this work. In instances where I am not the responsible author I have consulted with the responsible author to agree on the respective contributions of the authors.

CONTENTS

Main Supervisor name: Kimbal Marriott

Main Supervisor signature:

Date: 2021-12-12

Acknowledgments

I would like to express my sincere gratitude to my supervisors, professor Kimbal Marriott and professor Dianne Cook, for their support of my Ph.D studies and research, their subject expertise, and their careers of supervising and teaching in addition to performing research. Thank you for continuously pushing me and my research to new levels. I have enjoyed teaching data visualization, which has been strongly shaped by Di's practical, data-first, visualization-often pragmatic approach. I will continue to hearing Kim's persistent question "what do we learn from this?" as a reminder not to get lost in the details of implementation, but also to regularly step back and analyze if this is the correct object to change.

A special thanks to professor Przemyslaw Biecek for giving his input in the formulation stages of my project and his easy-to-understand explanations of complex modeling aspects. Thank you for responding to cold emails and being available for collaboration.

I thank my fellow Ph.D students, lab members, and Pomodoro partners especially on the occasional of stimulating discussions and for the positive peer pressure of knowing others are around and working. Thanks immensely to those who empathized with me and others, especially through the hardships of studies and COVID-19. Gratitude to Ying Zhou for her enduring support through the thick of my studies and wavering mental health.

Last but not least, I would like to thank my parents, Doug and Terry, for their support and concerns at odd hours of the day. Thanks to Alan and Claire for their companionship and support now and in our more formative years. I am looking forward to seeing you all in person shortly.

Preface

This thesis has been written using R Markdown with the bookdown package (Xie, 2016). All materials required to compile the thesis are available at https://github.com/nspyrison/thesis_monash_phd.

I recognize that terminology is often overburdened by ambiguous use, with several changing meanings coming from different fields. My background comes from Statistics and I will default to terms from statistics and geometry.

Chapter 2 has been published in *The R Journal*. Chapters 3 and 4 have not been submitted yet.

Chapter 1

Introduction

Exploratory Data Analysis (EDA) is the process of the initial summarization and visualization of a dataset. This is a critical first step of checking for realistic values, finding improper data formats, and revealing insights (Tukey, 1977). Early and frequent data visualization is key to the data analyst's workflow cycle (Wickham and Grolemund, 2017). As modern datasets grow in complexity use of multivariate data is ubiquitous. The number of variables in the data increases the difficulty of creating and portraying an accurate representation of the data, which is central to the iterated workflow.

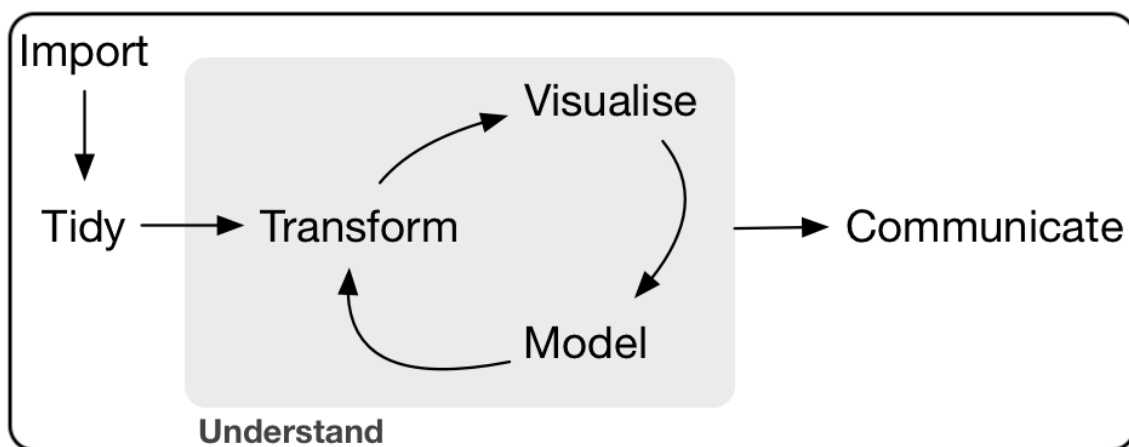


Figure 1.1: Data analysis workflow (Wickham and Grolemund, 2017). This work focuses primary on multivariate data visualization, but also facilitates transforming data and interpretation of models.

Early attempts at high-dimension visuals in scatterplot matrices (Chambers et al., 1983) and parallel coordinate plots (Ocagne, 1885). Principal component analysis (PCA, Pearson (1901)) reorients the basis to components, linear combinations of the original variables ordered by descending amount of variation explained. These components are typically viewed as discrete orthogonal pairs.

A data visualization *tour* (Cook et al., 2008; Lee et al., 2021) is a class of linear projections that animate small changes to the projection basis. Intuitively, they show a projection of the data object down to lower-dimensional space in the same way that a 3D object casts a 2D shadow. A key feature of the tour is the persistence and tractability of the points through many frames. In the shadow analogy an object, such as a bar stool may be casting a circular shadow that could come from any number of shapes. However, if the stool were rotated, the legs would show in the shadow quickly giving an intuitive interpretation of the object. Similarly, looking at a data object over the rotation of its variables yields information about its structure. In this way and aided with linked brushing and other interactions, such continuous tours excel at extending the interpretability of multivariate spaces. Chapter 1.4 walks through some of the previous alternatives and why we ultimately continue with this class of animated linear dimension reduction.

Component spaces and tours optimize for specific objectives or are selected randomly. None of the previous methods allow for an analyst to control the contributions of variables to the basis. This is a crucial component for *human-in-the-loop* analysis (Karwowski, 2006). If the analyst wants to explore what happens to the structure if one variable were removed or contribution of another was increased they had no way to do so.

1.1 Research questions

The over-arching question of interest can be stated as:

Can the radial tour with user interaction help analysts understand linear projections, and explore the sensitivity of structure in the projection to the variables contributing to the projection?

Understanding variable sensitivity to the structure in a projection frame is crucial factor analysis after identifying a feature of interest. If an identified feature is the *what* of an analysis then its variable attributions are its *how*. The user interaction afforded by the radial tour should allow for a more precise exploration of this structure.

RQ 1. How do we define user interaction for the radial tours to add and remove variables smoothly from a 2D linear projection of data?

Neither component spaces nor grand tour provide a means for changing the contributions of a desired variable. To facilitate variable interaction, we need to have a means of manipulating the basis. This is crucial to explore the sensitivity of the variable contributions to the structure in a frame.

RQ 2. Does the use of the radial tour improve analysts understanding of the relationship between variables and structure in 2D linear projections?

How can we be sure that having a means of control leads to a meaningfully better analysis? Comparing alternative methods should lend insight into which methods perform well under specific tasks.

RQ 3. Can the radial tours be used in conjunction with the local explanation, SHAP, to improve the interpretability of black-box models?

The tension from the trade-off between accuracy and interpretability of black-box models is rising. There is a clear need to be able to explain black-box models. After extrapolating local explanations of all observations, we want to explore that space with the help of the radial tour.

1.2 Methodology

The research corresponding with RQ #1 entails *algorithm/software design* adapting the algorithm from Cook and Buja (1997). This allows for interactive control of 2D projections and serves as a foundation for the remaining work.

To address RQ #2, a controlled *experimental study* has explored the efficacy of interactive radial tours as compared with two benchmark methods: Principal Component Analysis (PCA, Pearson (1901)) and the grand tour (Asimov, 1985). This was a within-participant

user study where each participant experienced each visual. Trials were balanced across three other experimental factors: location of the signal, the shape of the cluster distributions, and the dimensionality of the data. Ethics approval was obtained for this work. The approval and disclosure forms are available at the project repository: https://github.com/nspyrison/spinifex_study/tree/master/ethics.

The research for RQ #3 involves *fundamental visualization design*. We know that the SHAP value is a local explanation for one observation. This SHAP value will also serve as the 1D basis for the radial tour. While using SHAP as a projection basis is novel, it is not particularly insightful by itself. With the radial tour we can change variable contributions. We also provide linkage information, the within-class distributions of the SHAP components as parallel coordinate marks on the basis. We also offer a global view and related statistics to map to color to aid in exploring the sensitivity of the SHAP-space relative to the sensitivity of the original data space.

1.3 Contributions

1. **spinifex**, a package offering a consistent framework for performing radial tours and the rendering of any tours to various formats:
 - Perform radial tours to explore the variable sensitivity to structure
 - Transform numeric variable in the data
 - Extract various bases exposing features of the data
 - Interoperable with tours generated with **tour** (Wickham et al., 2011)
 - Layered interface for producing tours that mirror the layered approach of **ggplot2** (Wickham, 2016)
2. A user study comparing the efficacy of the radial tour against the alternatives of PCA the grand tour includes:
 - Creation of supervised classification task to assess the variable attribution to the separation of clusters performed under various levels of experimental factors: location, shape, and dimensionality.
 - Definition of an accuracy measure to evaluate this task.

- Results: strong evidence that the radial tour increases the accuracy of this task by a sizable amount while the task is performed fastest with the grand tour.
- Attribution of the error by performing a mixed model regression helps to explain the source of the error term into the variability of participants skill aptitude for this task and variability of the difficultly of a simulation by random chance.
- Introduces an interactive application to preprocess data and explore. Users can choose from six supplied datasets or upload their own.

3. **cheem**, a package applying the radial tour to local explanations of black-box models, including:

- Preprocessing; creation of a random forest model, the extraction of all observation's tree SHAP local explanation, and extraction of other statistics for display.
- Visualization of approximations of the data- and attribution-space side-by-side with linked brushing, hover tooltips, and tabular display of selected points.
- Evaluating the local explanations with the use of the radial tour we can explore the sensitivity to the structure identified better see what variable support the explanation holds realistic.

1.4 Background

This section starts with setting the scope for the type of data we are focusing on, gives a brief motivation then works through previous multivariate visualizations and their scalability. By the end, the focus narrows to linear projections, and in particular, the class of animated linear projections known as the tour.

For our purposes I will be focusing on the case where data $X_{n \times p}$ contains n observations of p variables, is complete with no missing values, variables are numeric (ideally not ordinal levels), and $n > p$ typically many more observations than variables. While I write as though always operating on the original variable space these methods could similarly be applied to feature decomposition of data not fitting this description. In the case of the linear projection let, $Y_{n \times d} = X_{n \times p} * A_{p \times d}$ be the embedding of the data mapped by the basis A , where $d < p$. When p is large, say over 10 or 20 variables, the viewing space is quite large. In these cases, a PCA initialization step is commonly used where the variables

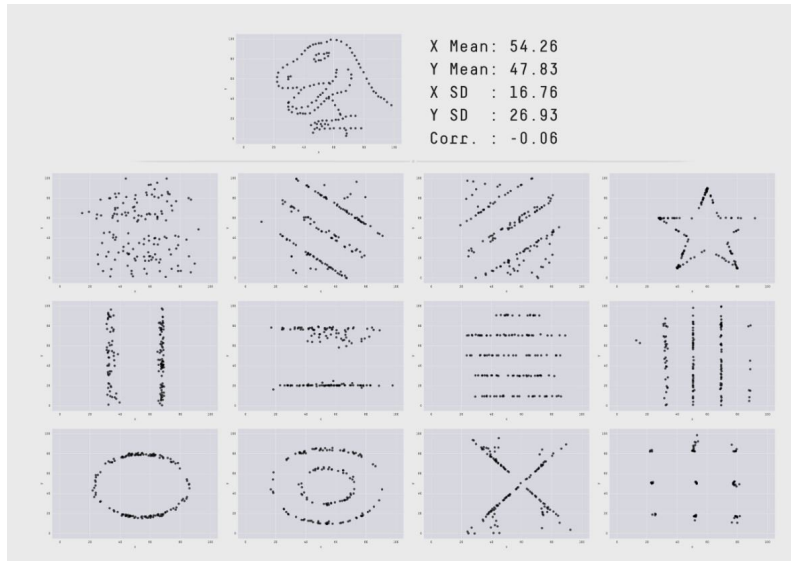


Figure 1.2: Starting from the profile of a dinosaur, observations are allowed to drift (by iterated simulated annealing) toward 12 patterns provided that they stay close to the original statistics (Matejka and Fitzmaurice, 2017). Visualization of data yields stark patterns that are easy to miss in numerical summarization.

are approximated as fewer principal components, and this reduced space can be viewed, albeit with the disadvantage of having another linear mapping back to the original space. Wickham, Cook, and Hofmann (2015) also view model spaces and features while urging to have a preference for visualizing data-space directly.

Visualization is much more robust than numerical summarization alone (Anscombe, 1973; Matejka and Fitzmaurice, 2017). In these studies, data sets have the same summary statistics, yet contains obvious visual trends and shapes that could go completely unheeded if plotting is foregone. Data visualization is fundamental to EDA and quickly evaluating data supports ensuring that models are suitable.

1.4.1 Scatterplot matrices

The work in Grinstein, Trutschl, and Cvek (2002) gives a good taxonomy of high-dimensional visualization. We will follow a few examples building up to why we conclude with tour methods. Broadly speaking, we are concerned with the question “How can an analyst visualize arbitrary p - dimensions?”. To illustrate some of the options for data I use the penguins data(Gorman, Williams, and Fraser, 2014, horst_palmerpenguins_2020). It

contains 333 observations of four physical measurements across three species of penguins observed near Palm Station, Antarctica.

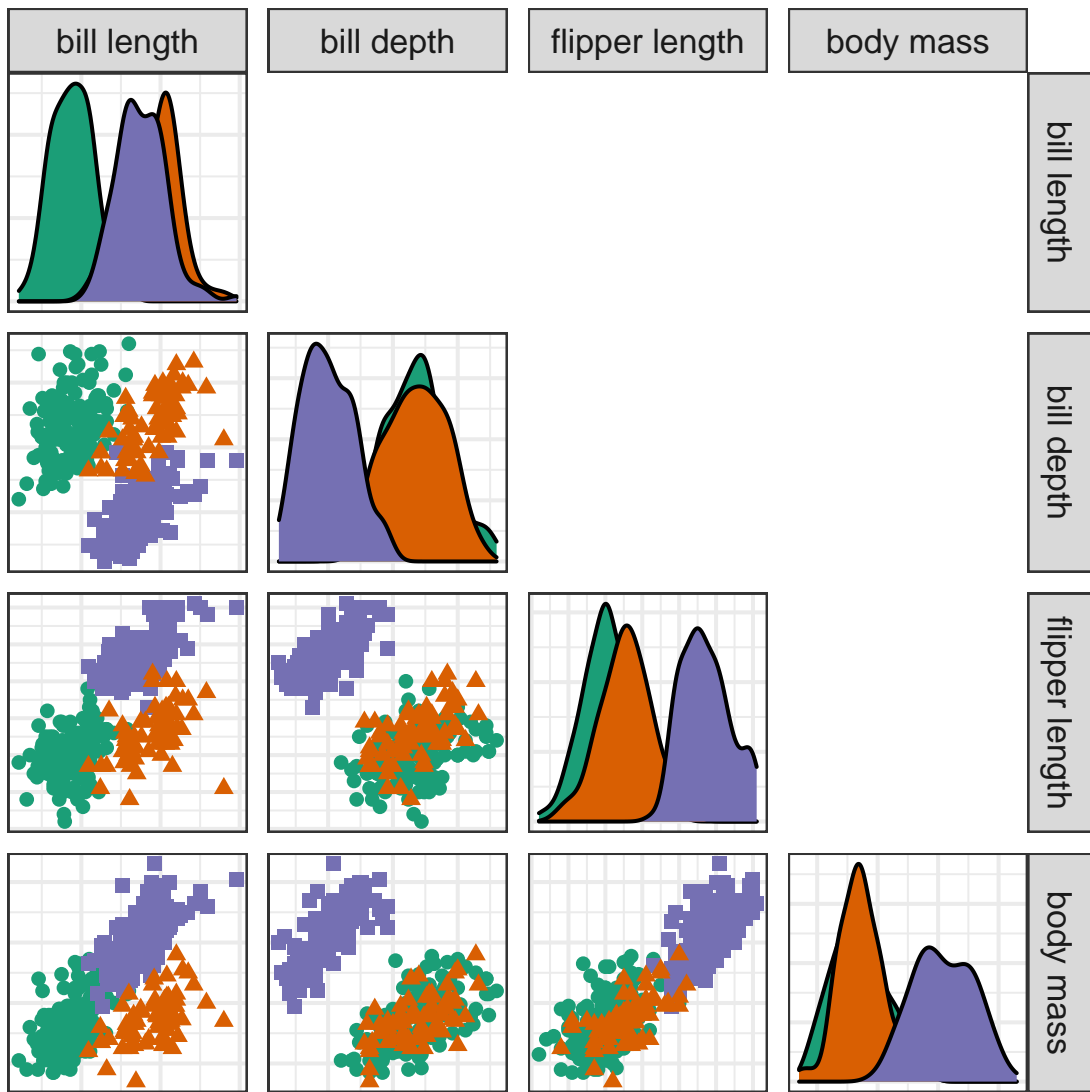
Viewing as many univariate histograms or density curves is one method. Similarly, one could look at all variable pairing as scatter plots. This forms the crux of the scatterplot matrices, also known as SPLOM (Chambers et al., 1983). In a scatterplot matrix, variables are displayed across the columns and rows, the diagonal elements show the univariate densities while off-diagonal positions show scatterplot pairs. This is useful for getting a handle on the support and shapes of the variables, but is not going to scale well with dimension and is not a suitable audience-ready display as it is very busy and doesn't draw attention to any one spot. Munzner reminds us to abstract all of the cognitive work out of the visual, allowing the audience to focus on seeing the evidence supporting the claim (Munzner, 2014).

1.4.2 Parallel coordinate plots

Alternatively, we could consider a class of observation-based visuals. In parallel coordinate plots (Ocagne, 1885) variables are arranged horizontally and observations are connected by lines with the height mapping to the quantile or z-value for each variable. This scales much better with dimensions but poorly with observations. It also suffers from an asymmetry with the variable order, that is, changing the order of the variable will lead people to very different conclusions. The x-axis is also used to display variables rather than the values of the observations. This restricts the amount of information that can be interpreted between variables. Munzner asserts that position is the more human-perceptible channel for encoding information; we should like to reserve it for the values of the observations. The same issues persist across other observation-based displays such as radial variants, pixel-oriented visuals, and Chernoff faces (Keim, 2000; Chernoff, 1973). These visuals are better suited for the $n < p$ case with more variables than observations.

1.4.3 Dimension reduction

Ultimately, we will need to turn to dimension reduction to create a compelling visual allowing audiences to focus on features with contributions from multiple variables. Dimension

**Figure 1.3:** (*ref:penguinsmplom-cap*)

reduction is separated into two categories, linear and non-linear. The linear case spans all affine mathematical transformations, essentially any mapping where parallel lines stay parallel. Non-linear transformations are the complement of the linear case, think transformations containing exponents or interacting terms. Examples in low dimensions are relatable. For instance, shadows are examples of linear projections where a 3-dimensional object casts a 2D projection, the shadow. Our vision at any one instance of time, or a picture, are also a 2D projections. An example of a non-linear transformation is that of 2D representation of the globe. There are many different ways (and features to optimize) to distort the surface to display as a map. The most common may be rectangular displays

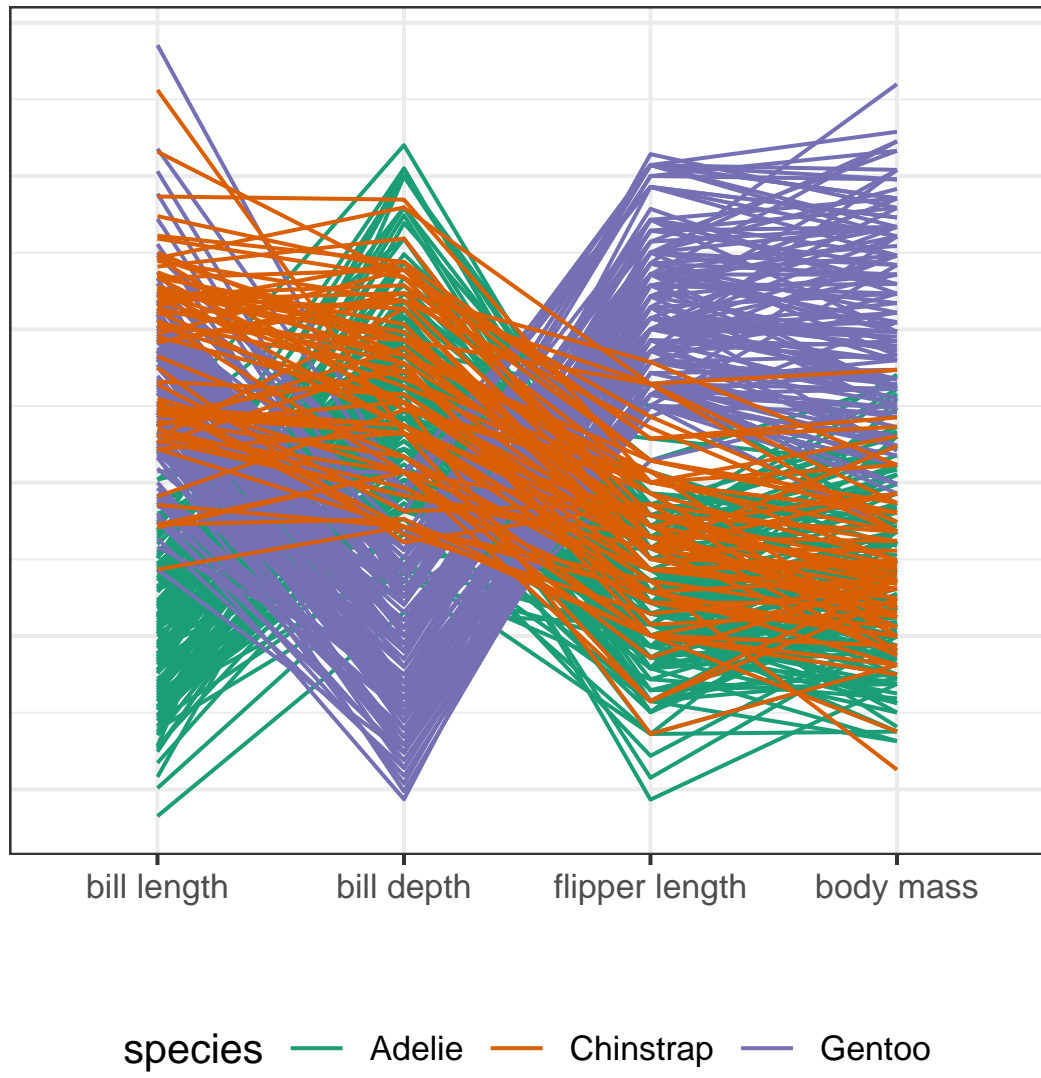


Figure 1.4: Parallel coordinate plots of penguins data. Does not scale well with observations and suffers from asymmetry with the variable ordering, and horizontal position is used for variable rather than observation levels.

where the area is distorted more and more with the distance away from the equator. Other distortions are created when the surface is unwrapped as a long ellipse. Yet others create non-continuous gaps in oceans to minimize the distortion of countries.

Non-linear techniques often have hyperparameters that affect how the spaces are distorted to fit into a fewer dimensions. To quote Anastasios Panagiotelis, “All non-linear projections are wrong, but some are useful”, a play on George Box’s quote about models. Non-linear techniques distort the space in unclear ways, and what is more, they can introduce features not in the data depending on the selection of hyperparameters. The presence of structure in a non-linear model is necessary but not sufficient to conclude the existence of a structure in the data.

Unfortunately, there is no free lunch here. An increase in the original data dimensions will lead to a $p - d$ -dimensional viewing space in the linear case, and an increasingly perturbed and distorted space in non-linear techniques. The intrinsic dimensionality of data is the number of variables needed to minimally represent the data (Grinstein, Trutschl, and Cvek, 2002). This is an important aspect of dimension reduction that does not have to end in visual, but is also a common part of factor analysis and preprocessing data. Consider a Psychology survey consisting of 100 questions about the Big Five personality traits. The data consists of 100 variables, while the theory would suggest the intrinsic dimensionality is five. The data likely picks up on other aspects and may better be summarized in with eight or ten dimensions. If this were the case, reducing the data to this space would be necessary to gate the exponentially increasing view time.

1.4.4 Tours, animated linear projections

A single linear projection is a resulting space from the data multiplied by the basis where the basis is an orthonormal matrix (the orientation of the unit origin) mapping the data space to a lower dimension. A data visualization tour animates many such projections through small changes in the basis. In the bar stool shadow analogy, structural information about a hidden object was gained by watching its shadow change due to its rotation. An analyst similarly gains information about the data object by watching continuous changes

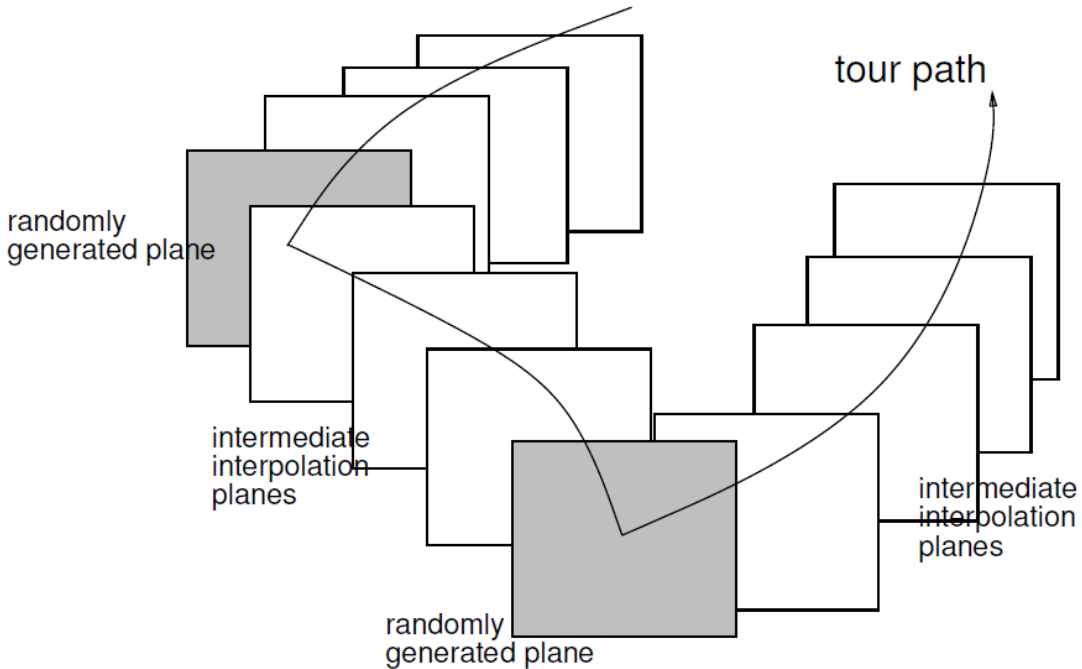


Figure 1.5: Illustration of the grand tour selecting random target frames (grey) connected via geodesically interpolated frame (white). Figure from Buja et al. (2005).

to the basis (the rotation of the data). Originally in a *grand tour* (Asimov, 1985) several target frames are randomly selected and then interpolated along their geodesic path.

There are various types of tours which are classified by the generation of their basis paths. A *guided* tour uses simulated annealing to move progressively closer to an objective function in the embedded space (Hurley and Buja, 1990). A more comprehensive discussion and review of tours can be found in the works of Cook et al. (2008) and Lee et al. (2021).

Tours are used for a couple of salient features: maintains transparency back to the original variable space, and the persistence data points from frame to frame convey more information than looking at discrete jumps to other bases. Because of these features, tours are a good method to extend the visualization of data space as dimensionality increases.

The work below covers manual tours (Cook and Buja, 1997; Spyrlis and Cook, 2020) in Chapter 2. Radial tours are one type of manual tour that where the contribution of one variable is extended radially to a full contribution, removed completely, then restored to its original contribution. Chapter 3 compares the efficacy of the radial tour as compared

with PCA and the grand tour in a user study. Lastly, Chapter 4 extends the use of the radial tour to evaluate the local explanation of black-box models.

1.5 Thesis structure

The remainder of the thesis is organized as follows: Chapter 2 discusses the theory and implementation of the manual tour in the package **spinifex**. Chapter 3 discusses a user study evaluating the efficacy of the radial, manual tour as compared with PCA and the grand tour. There is ample evidence that using the radial tour increases the accuracy of responses for the supervised variable-attribution task describing the separation between two variables. Chapter 4 extends the use of manual tours to improve the interpretability of non-linear models. Where manual tours explore variable sensitivity to the structure identified in local explanations of the model. Lastly, Chapter 5 concludes with some takeaways and a discussion of possible extensions.

Chapter 2

spinifex: an R package for creating user-controlled animated linear projections

This chapter introduces manual tours that allows analysts to influence the contributions to a projection. This feature is absent from previous linear embeddings. This work has changed from its publication, primarily to incorporate and discuss the subsequent ‘ggproto’ API that extends the flexibility of the geometric displays of tours.

Dynamic low-dimensional linear projections of multivariate data known as *tour* provide an essential tool for exploring multivariate data and models. The R package **tourr** provides functions for several types of tours: grand, guided, little, local, and frozen. Each of these can be viewed in a development environment, or their basis array can be saved for later consumption. This paper describes a new package, **spinifex**, which provides a manual tour of multivariate data. In a manual tour an analyst controls the contribution of a variable to the projection. Controlled manipulation is important to explore a variables sensitivity to structure of an identified feature. The use of the manual tour is applied to particle physics data to illustrate the sensitivity of structure in a projection to specific variable contributions. Additionally, we create a ‘ggproto’ API for composing any tour that mirrors

the layered additive approach of **ggplot2**. Tours can then be animated and exported to various formats with **plotly** or **gganimate**.

2.1 Introduction

Exploring multivariate spaces is a challenging task, increasingly so as dimensionality increases. Traditionally, static low-dimensional projections are used to display multivariate data in two dimensions, including principal component analysis, linear discriminant spaces or projection pursuit. These are useful for finding relationships between multiple variables, but they are limited because they show only a glimpse of the high-dimensional space. An alternative approach is to use a tour (Asimov, 1985) of dynamic linear projections to look at many different low-dimensional projections. Tours can be considered to extend the dimensionality of visualization, which is important as data and models exist in more than three dimensions. The package **tourr** (Wickham et al., 2011) provides a platform for generating tours. It can produce a variety of tours, each paired with a variety of possible displays. A user can make a grand, guided, little, local or frozen tour, and display the resulting projected data as a scatterplot, density plot, histogram, or even as Chernoff faces if the projection dimension is more than 3.

This work adds a manual tour to the collection. The manual tour was described in Cook and Buja (1997) and allows a user to control the projection coefficients of a selected variable in a 2D projection. The manipulation of these coefficients enable the analyst to explore their sensitivity to the structure within the projection. As manual tours operate on only one variable, they are particularly useful once a feature of interest has been identified.

One way to identify “interesting” features is using a guided tour (Cook et al., 1995). Guided tours select a very specific path, which approaches a projection that optimizes an objective function. The optimization used to guide the tour is simulated annealing (Kirkpatrick, Gelatt, and Vecchi, 1983). The direct optimization of a function allows guided tours to rapidly identify interesting projection features given the relatively large parameter-space. After a projection of interest is identified, an analyst can then use the “finer brush” of the manual tour to control the contributions of individual variables to explore the sensitivity they have on the structure visible in the projection.

The paper is organized as follows. Section 2.2 describes the algorithm used to perform a radial manual tour implemented in the package **spinifex**. Section 2.3 discussed the functions, their usage composing tours with **ggplot2** (Wickham, 2016) and their animation by **plotly** (Sievert, 2020) or **ggridge** (Pedersen and Robinson, 2020). Package functionality and code usage following the order applied in the algorithm follows in section 2.3.2. Section 2.4 illustrates how this can be used for sensitivity analysis applied to multivariate data collected on high-energy physics experiments (Wang et al., 2018). Section 2.5 summarizes this paper and discusses potential future directions.

2.2 Algorithm

The algorithm to conduct a manual tour interactively by recording mouse/cursor motion is described in detail in Cook and Buja (1997). Movement can be in any direction and magnitude, but it can also be constrained in several ways:

- *radial*: fix the direction of contribution, and allow the magnitude to change.
- *angular*: fix the magnitude, and allow the angle or direction of the contribution to vary.
- *horizontal, vertical*: allow rotation only around the horizontal or vertical axis of the current 2D projection.

The algorithm described here produces a **radial** tour as an *animation sequence*. It takes the current contribution of the chosen variable, and using rotation brings this variable fully into the projection, completely removes it, before returning to the original position.

2.2.1 Notation

The notation used to describe the algorithm for a 2D radial manual tour is as follows:

- **X**, the data, an $n \times p$ numeric matrix to be projected.
- **A**, any orthonormal projection basis, $p \times d$ matrix, describing the projection from $\mathbb{R}^p \Rightarrow \mathbb{R}^d$.
- k , is the index of the manipulation variable or manip var for short.

- \mathbf{e} , a 1D basis vector of length p , with 1 in the k -th position and 0 elsewhere.
- \mathbf{M} is a $p \times 3$ matrix, defining the 3D subspace where data rotation occurs and is called the manip(ulation) space.
- \mathbf{R} , the $d + 1$ -D rotation matrix, for performing unconstrained 3D rotations within the manip space, \mathbf{M} .
- θ , the angle of in-projection rotation, for example, on the reference axes; c_θ, s_θ are its cosine and sine.
- ϕ , the angle of out-of-projection rotation, into the manip space; c_ϕ, s_ϕ are its cosine and sine. The initial value for animation purposes is ϕ_1 .
- \mathbf{U} , the axis of rotation for out-of-projection rotation orthogonal to \mathbf{e} .
- $\mathbf{Y} = \mathbf{X} \times \mathbf{A}$, the resulting projection of the data through the manip space, \mathbf{M} , and rotation matrix, \mathbf{R} .

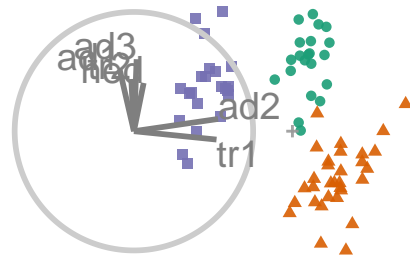
The algorithm operates entirely on projection bases and incorporates the data only when making the projected data plots in light of efficiency.

2.2.2 Steps

Step 0) Setup

The flea data (Lubischew (1962)), available in the **tourr** package, is used to illustrate the algorithm. The data contains 74 observations of six variables, physical measurements of flea beetles. Each observation belongs to one of three species.

An initial 2D projection basis must be provided. A suggested way to start is to identify an interesting projection using a projection pursuit guided tour. Here the holes index is used to find a 2D projection of the flea data, which shows three separated species groups. Figure 2.1 shows the initial projection of the data. The left panel displays the projection basis (\mathbf{B}) and can be used as a visual guide of the magnitude and direction that each variable contributes to the projection. The right panel shows the projected data, $\mathbf{Y}_{[n, 2]} = \mathbf{X}_{[n, p]} \mathbf{B}_{[p, 2]}$. The color and shape of points are mapped to the flea species.



colour	● Concinnia	● Heikert.	● Heptapot.
shape	● Concinnia	▲ Heikert.	■ Heptapot.

Figure 2.1: Biplot of the initial 2D projection: representation of the basis (left) and resulting data projection (right) of standardized flea data. The color and shape of data points are mapped to the species of flea beetle. The basis was produced by a projection pursuit guided tour with the holes index. The contribution of the variables *aede2* and *tars1* approximately contrasts the other variables. The visible structure in the projection are the three clusters corresponding to the three species.

Step 1) Choose manip variable

In figure 2.1 the contribution of the variables *tars1* and *aede2* mostly contrast the contribution of the other four variables. These two variables combined contribute in the direction of the projection where the purple cluster is separated from the other two clusters. The variable *aede2* is selected as the manip var, the variable to be controlled in the tour. The question that will be explored is: how important is this variable to the separation of the clusters in this projection?

Step 2) Create the 3D manip space

Initialize the coordinate basis vector as a zero vector, \mathbf{e} , of length p , and set the k -th element to 1. In the example data, *aede2* is the fifth variable in the data, so $k = 5$, set $e_5 = 1$. Use a Gram-Schmidt process to orthonormalize the coordinate basis vector on the original 2D projection to describe a 3D manip space, \mathbf{M} .

$$e_k \leftarrow 1$$

$$\mathbf{e}_{[p, 1]}^* = \mathbf{e} - \langle \mathbf{e}, \mathbf{B}_1 \rangle \mathbf{B}_1 - \langle \mathbf{e}, \mathbf{B}_2 \rangle \mathbf{B}_2$$

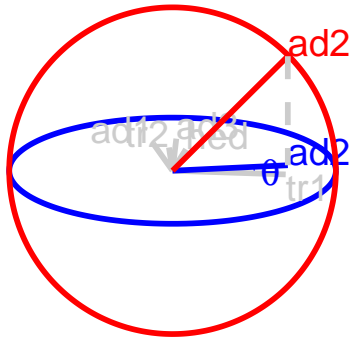


Figure 2.2: Illustration of a 3D manip space, the projection plane is shown as a blue circle extending into and out of the display. A manipulation direction is initialized, the red circle, orthogonal to the projection plane. This allows the selected variable, `aede2`, to change its contribution back to the projection plane. The other variables contributions rotate into this space as well, preserving the orthogonal structure, but are omitted in the manipulation dimension for simplicity.

$$\mathbf{M}_{[p, 3]} = (\mathbf{B}_1, \mathbf{B}_2, \mathbf{e}^*)$$

The manip space provides a 3D projection from p -dimensional space, where the coefficient of the manip var can range completely between [0, 1]. This 3D space serves as the medium to rotate the projection basis relative to the selected manipulation variable. Figure 2.2 illustrates this 3D manip space with the manip var highlighted. This representation is produced by calling the `view_manip_space()` function. This diagram is purely used to help explain the algorithm.

Step 3) Defining a 3D rotation

The basis vector corresponding to the manip var (red line in Figure 2.2), can be operated like a lever anchored to the origin. This is the process of the manual control, that rotates the manip variable into and out of the 2D projection (Figure 2.3). As the variable contribution is controlled, the manip space turns, and the projection onto the horizontal projection plane correspondingly changes. This is a manual tour. Generating a sequence of values for the rotation angles produces a path for the rotation of the manip space.

For a radial tour, fix θ , the angle describing rotation within the projection plane, and compute a sequence for ϕ , defining movement out of the plane. This will change ϕ from

the initial value, ϕ_1 , the angle between \mathbf{e} and its shadow in \mathbf{B} , to a maximum of 0 (manip var fully in projection), then to a minimum of $\pi/2$ (manip var out of projection), before returning to ϕ_1 .

Rotations in 3D can be defined by the axes they pivot on. Rotation within the projection, θ , is rotation around the Z -axis. Out-of-projection rotation, ϕ , is the rotation around an axis on the XY plane, \mathbf{U} , orthogonal to \mathbf{e} . Given these axes, the rotation matrix, \mathbf{R} , can be written as follows, using Rodrigues' rotation formula (originally published in Rodrigues (1840)):

$$\begin{aligned}\mathbf{R}_{[3, 3]} &= \mathbf{I}_3 + s_\phi \mathbf{U} + (1 - c_\phi) \mathbf{U}^2 \\ &= \begin{bmatrix} 1 & 0 & 0 \\ 0 & 1 & 0 \\ 0 & 0 & 1 \end{bmatrix} + \begin{bmatrix} 0 & 0 & c_\theta s_\phi \\ 0 & 0 & s_\theta s_\phi \\ -c_\theta s_\phi & -s_\theta s_\phi & 0 \end{bmatrix} + \begin{bmatrix} -c_\theta(1 - c_\phi) & s_\theta^2(1 - c_\phi) & 0 \\ -c_\theta s_\theta(1 - c_\phi) & -s_\theta^2(1 - c_\phi) & 0 \\ 0 & 0 & c_\phi - 1 \end{bmatrix} \\ &= \begin{bmatrix} c_\theta^2 c_\phi + s_\theta^2 & -c_\theta s_\theta(1 - c_\phi) & -c_\theta s_\phi \\ -c_\theta s_\theta(1 - c_\phi) & s_\theta^2 c_\phi + c_\theta^2 & -s_\theta s_\phi \\ c_\theta s_\phi & s_\theta s_\phi & c_\phi \end{bmatrix}\end{aligned}$$

where

$$\begin{aligned}\mathbf{U} &= (u_x, u_y, u_z) = (s_\theta, -c_\theta, 0) \\ &= \begin{bmatrix} 0 & -u_z & u_y \\ u_z & 0 & -u_x \\ -u_y & u_x & 0 \end{bmatrix} = \begin{bmatrix} 0 & 0 & -c_\theta \\ 0 & 0 & -s_\theta \\ c_\theta & s_\theta & 0 \end{bmatrix}\end{aligned}$$

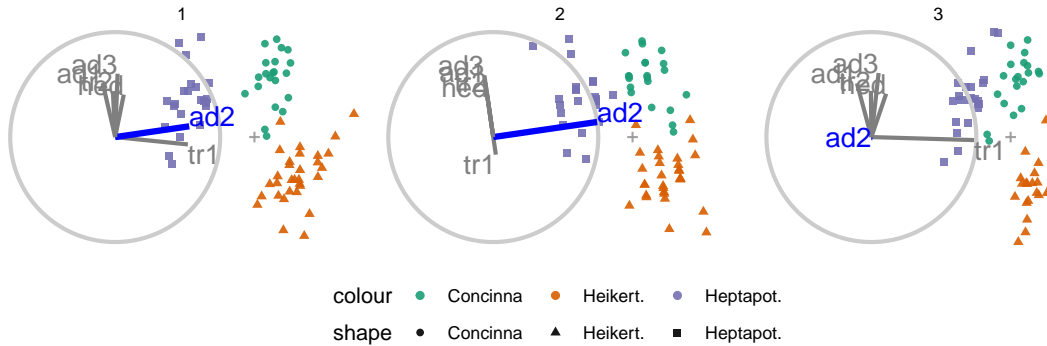


Figure 2.3: Select frames highlight the animation of a radial manual tour manipulating *aede2*: (1) original projection, (2) full contribution, (3) zero contribution, before returning to the original contribution.

Step 4) Creating an animation of the radial rotation

The steps outlined above can be used to create any arbitrary rotation in the manip space. To use these for sensitivity analysis, the radial rotation is built into an animation where the manip var is rotated fully into the projection, completely out, and then back to the initial value. This involves allowing ϕ to vary between 0 and $\pi/2$, call the steps ϕ_i .

1. Set initial value of ϕ_1 and θ : $\phi_1 = \cos^{-1} \sqrt{B_{k1}^2 + B_{k2}^2}$, $\theta = \tan^{-1} \frac{B_{k2}}{B_{k1}}$. Where ϕ_1 is the angle between **e** and its shadow in **B**.
2. Set an angle increment (Δ_ϕ) that sets the step size for the animation, to rotate the manip var into and out of the projection. Uses of angle increment, rather than a number of steps to control the movement is consistent with the tour algorithm as implemented in the **tourr**.
3. Step towards 0, where the manip var is entirely in the projection plane.
4. Step towards $\pi/2$, where the manip variable has no contribution to the projection.
5. Step back to ϕ_1 .

In each of the steps 3-5, a small step may be added to ensure that the endpoints of $\phi(0, \pi/2, \phi_1)$ is reached.

Step 5) Projecting the data

The operation of a manual tour is defined on the projection bases. Only when the data plot needs to be made the data projected into the relevant basis.

$$\mathbf{Y}_{[n, 3]}^{(i)} = \mathbf{X}_{[n, p]} \mathbf{M}_{[p, 3]} \mathbf{R}_{[3,3]}^{(i)}$$

where $\mathbf{R}_{[3,3]}^{(i)}$ is the incremental rotation matrix, using ϕ_i . To make the data plot, use the first two columns of \mathbf{Y} . Show the projected data for each frame in sequence to form an animation.

Tours are typically viewed as an animation. The animation of this tour can be viewed online on [GitHub](#). The page may take a moment to load.

2.3 Package structure

This section describes the functions available in the package, their usage, and how to install and get up and running.

2.3.1 Functions

Table 2.1 lists the primary functions and their purpose. These are grouped into four types: processing the data, production of tour path, the composition of the tour display, and its animation.

2.3.2 Usage

Using the penguins data , available in the package, to illustrate a manual tour, we will illustrate generating a manual tour to explore the sensitivity of a variable separating two clusters. The composition of the tour display echos the additive layered approach of

Table 2.1: Summary of primary functions.

Family	Function	Related to	Description
processing	scale_01/sd	-	scale each column to [0,1]/std dev away from the mean
processing	basis_pca/olda/...	Rdimtools::do.*	basis of orthogonal component spaces
processing	basis_half_circle	-	basis with uniform contribution across half of a circle
processing	basis_guided	tourr::guided_tour	silently return the basis from a guided tour
tour path	manual_tour	-	basis and interpolation information for a manual tour
tour path	save_history	tourr::save_history	silent, extended wrapper returning other tour arrays
display	ggtour	ggplot2::ggplot	canvas and initialization for a tour animation
display	proto_point/text	geom_point/text	adds observation points/text
display	proto_density/2d	geom_density/2d	adds density curve/2d contours
display	proto_hex	geom_hex	adds hexagonal heatmap of observations
display	proto_basis/1d	-	adds adding basis visual in a unit-circle/-rectangle
display	proto_origin/1d	-	adds reference mark in the center of the data
display	proto_default/1d	-	wrapper for proto_* point + basis + origin
display	facet_wrap_tour	ggplot2::facet_wrap	facets on the levels of variable
display	append_fixed_y	-	add/overwrite a fixed vertical position
animation	animate_plotly	plotly::ggplotly	render as an interactive hmtl widget
animation	animate_gganimate	gganimate::animate	render as a .gif, .mp4, or other video format
animation	filmstrip	-	static ggplot faceting on the frames of the animation

ggplot2, while abstracting away the complexity of dealing with changing number of frames and their animation.

```
## Process penguins data

dat      <- scale_sd(penguins[1:4])
clas     <- penguins$species
bas      <- basis_olda(data = dat, class = clas)

## The tour path of the bases

mt_path <- manual_tour(basis = bas, manip_var = 1, data = dat)

## Composing the display of the tour

ggt <- ggtour(mt_path, angle = .15) +
  proto_point(aes_args      = list(color = clas, shape = clas),
              identity_args = list(alpa = .8, size = 1.5)) +
  proto_basis("left") +
  proto_origin()

## Animating

animate_plotly(ggt, fps = 10)
```

2.3.3 Installation

The `spinifex` is available from CRAN, the following code will help to get up and running:

```
# Installation:  
  
install.package("spinifex") ## Install from CRAN  
library("spinifex") ## Load into session  
  
# Getting started:  
## Shiny app for visualizing basic application  
run_app("intro")  
## View the code vignette  
vignette("getting_started_with_spinifex")  
## More about proto_* functions  
vignette("ggproto_api")
```

2.4 Use cases

Wang et al. (2018) introduce a new tool, PDFSense, to visualize the sensitivity of hadronic experiments to nucleon structure. The parameter-space of these experiments lies in 56 dimensions, and are approximated as the ten first principal components.

Cook, Laa, and Valencia (2018) illustrates how to learn more about the structures using a grand tour. Tours can better resolve the shape of clusters, intra-cluster detail, and better outlier detection than PDFSense & TFEP (TensorFlow embedded projections) or traditional static embeddings. This example builds from here, illustrating how the manual tour can be used to examine the sensitivity of structure in a projection to different parameters. The specific 2D projections passed to the manual tour were provided in their work.

The data has a hierarchical structure with top-level clusters; DIS, VBP, and jet. Each cluster is a particular class of experiments, each with many experimental datasets which each have many observations of their own. In consideration of data density, we conduct

manual tours on subsets of the DIS and jet clusters. This explores the sensitivity of the structure to each of the variables in turn and we present the subjectively best and worst variable to manipulate for identifying dimensionality of the clusters and describing the span of the clusters.

2.4.1 Jet cluster

The jet cluster resides in a smaller dimensionality than the full set of experiments, with four principal components explaining 95% of the variation in the cluster (Cook, Laa, and Valencia, 2018). The data within this 4D embedding is further subset to ATLAS7old and ATLAS7new, to focus on two groups that occupy different parts of the subspace. Radial manual tours controlling contributions from PC4 and PC3 are shown in Figures 2.4 and 2.5, respectively. The difference in shape can be interpreted as the experiments probing different phase spaces. Back-transforming the principal components to the original variables can be done for a more detailed interpretation.

When PC4 is removed from the projection (Figure 2.4), the difference between the two groups is removed, indicating that PC4 is essential for the separation of experiments. However, eliminating PC3 from the projection (Figure 2.5) does not affect the structure, meaning PC3 is not important for distinguishing experiments. Animations for the remaining PCs can be viewed at the following links: [PC1](#), [PC2](#), [PC3](#), and [PC4](#). It can be seen that only PC4 is important for viewing the difference in these two experiments.

2.4.2 DIS cluster

Following Cook, Laa, and Valencia (2018), to explore the DIS cluster, PCA is recomputed and the first six principal components, explaining 48% of the full sample variation, are used. The contributions of PC6 and PC2 are explored in Figures 2.6 and 2.7, respectively. Three experiments are examined: DIS HERA1+2 (green), dimuon SIDIS (purple), and charm SIDIS (orange).

Both PC2 and PC6 contribute to the projection similarly. When PC6 is rotated into the projection, variation in the DIS HERA1+2 is greatly reduced. When PC2 is removed from the projection, dimuon SIDIS becomes more distinct. Even though both variables

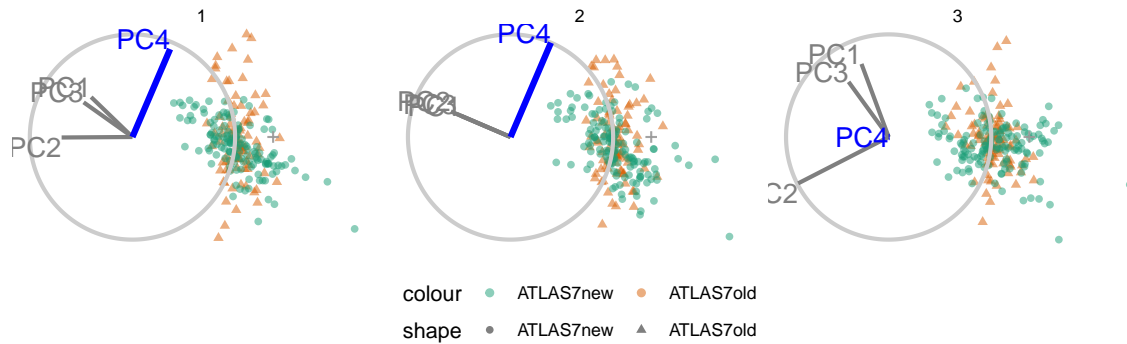


Figure 2.4: Select frames from a radial tour of PC4 within the jet cluster, with color indicating experiment type: ATLAS7new (green) and ATLAS7old (orange). When PC4 is removed from the projection (frame 10), there is little difference between the clusters, suggesting that PC4 is important for distinguishing the experiments.

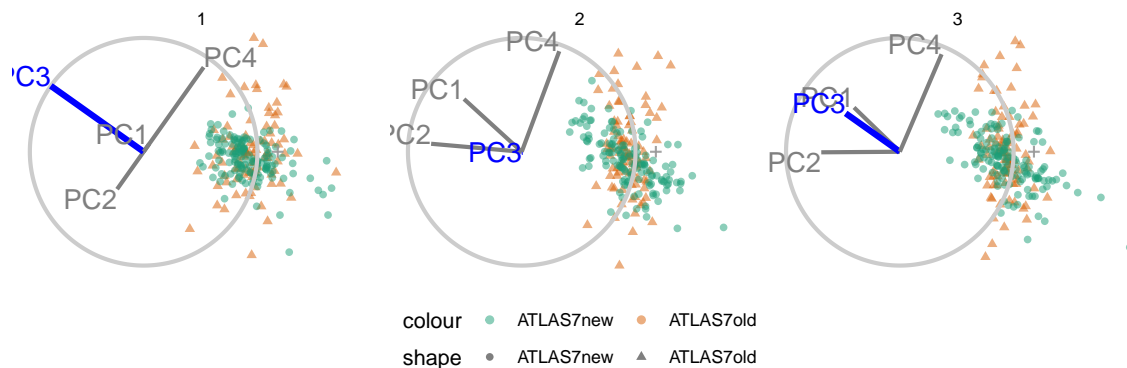


Figure 2.5: Frames from the radial tour manipulating PC3 within the jet cluster, with color indicating experiment type: ATLAS7new (green) and ATLAS7old (orange). When the contribution from PC3 is changed, there is little change in the separation of the clusters, suggesting that PC3 is not important for distinguishing the experiments.

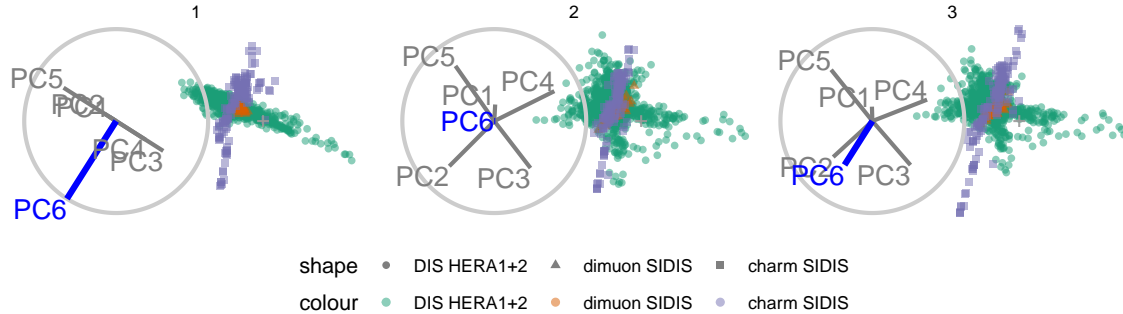


Figure 2.6: Select frames from a radial tour exploring the sensitivity that PC_6 has on the structure of the DIS cluster, with color indicating experiment type: DIS $HERA1+2$ (green), dimuon $SIDIS$ (purple), and charm $SIDIS$ (orange). DIS $HERA1+2$ is distributed in a cross-shaped plane, and charm $SIDIS$ occupies the center of this cross, and dimuon $SIDIS$ is a linear cluster crossing DIS $HERA1+2$. As the contribution of PC_6 is increased, DIS $HERA1+2$ becomes almost singular in one direction (frame 5), indicating that this cluster has very little variability in the direction of PC_6 .

contribute similarly to the original projection their contributions have quite different effects on the structure of each cluster, and the distinction between clusters. Animations of all of the principal components can be viewed from the links: [PC1](#), [PC2](#), [PC3](#), [PC4](#), [PC5](#), and [PC6](#).

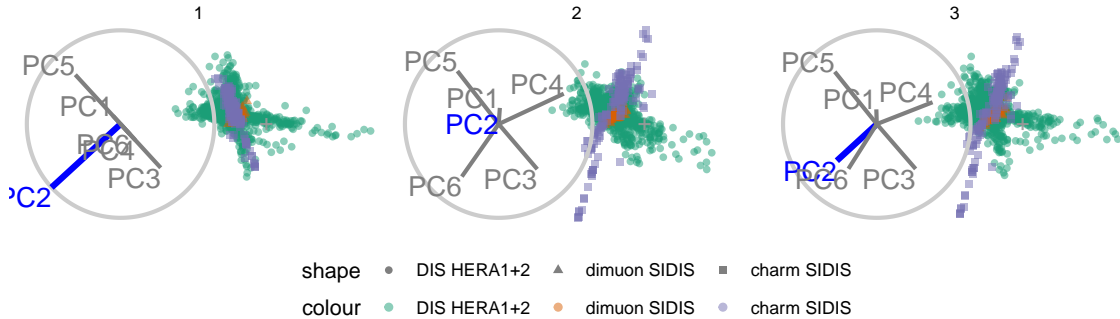


Figure 2.7: Frames from the radial tour exploring the sensitivity PC_2 to the structure of the DIS cluster, with color indicating experiment type: DIS HERA1+2 (green), dimuon SIDIS (purple), and charm SIDIS (orange). As the contribution of PC_2 is decreased, dimuon SIDIS becomes more distinguishable from the other two clusters, indicating that in the absence of PC_2 is important for separating this cluster from the others.

2.5 Discussion

Dynamic linear projections of numeric multivariate data, tours, play an important role in data visualization; they extend the dimensionality of visuals to peek into high-dimensional data and parameter spaces. This research has taken the manual tour algorithm, specifically the radial rotation, used in GGobi (Swayne et al., 2003) to interactively rotate a variable into or out of a 2D projection, and modified it to create an animation that performs the same task. It is most useful for examining the importance of variables and how the structure in the projection is sensitive or not to specific variables. This functionality is made available in the package **spinifex**. Which also extends the geometric display and export formats interoperable with the **tourr** package.

This work was motivated by problems in physics, and thus the usage was illustrated on data comparing experiments of hadronic collisions to explore the sensitivity of cluster structure to different principal components. These tools can be applied quite broadly to many multivariate data analysis problems.

The manual tour is constrained in the sense that the effect of one variable is dependent on the contributions of other variables in the manip space. However, this can be useful to simplify a projection by removing variables without affecting the visible structure. Defining a manual rotation in high dimensions is possible using Givens rotations and Householder reflections as outlined in Buja et al. (2005). This would provide more flexible manual rotation but more difficult for a user because they have the choice (too much choice) of which directions to move.

Another future research topic could be to extend the algorithm for use on 3D projections. With the current popularity and availability of 3D virtual displays, this may benefit the detection and understanding of the higher dimensional structure or enable the examination of functions.

Having a graphical user interface would be useful for making it easier and more accessible to a general audience. This is possible to implement using **shiny** (Chang et al., 2020). The primary purposes of the interface would be to allow the user to interactively change the manip variable easily and the interpolation step for more or less detailed views.

2.6 Acknowledgments

This article was created in R, using **knitr** (Xie, 2020) and **rmarkdown** (Allaire et al., 2020), with code generating the examples inline. The source files for this article be found at github.com/nspyrison/spinifex_paper/. The animated gifs can also be viewed at this site. The source code for the **spinifex** package can be found at github.com/nspyrison/spinifex/.

Chapter 3

The benefit of user-controlled radial tour for understanding variable contributions to structure in linear projections

Now we have the means to perform radial tours. Should we be confident that this method with user control will lead to better analysis than traditional alternatives? This chapter discusses the user study to elucidate the efficacy of the radial tour.

Principal component analysis is a long-standing go-to method for exploring multivariate data. Data visualization *tours* are a class of linear projections animated over small changes in the projection basis. The grand tour original selects target bases at random to animate between. Alternatively, the manual tour rotates the contribution of a selected variable novelly offering analysts a means to control the basis. This paper describes a within-participants user study evaluating the radial tour's efficacy compared with principal component analysis and the grand tour. We devise a supervised classification task where participants evaluate variable attribution of the separation between two classes. We define an accuracy measure as the response variable. Data were collected from 108 crowdsourced participants, who performed two trials of each visual for 648 trials in total. Mixed

model regression provides strong evidence that the radial tour increases accuracy over the alternatives. Participants subjectively prefer the use of the radial tour.

3.1 Introduction

Multivariate data is ubiquitous though its visualization quickly becomes complex. At the same time, we know that data visualization is imperative for Exploratory Data Analysis, (EDA, Tukey, 1977), the initial data summarization and testing model assumptions. Data visualization is more robust and informative than statistical summarization alone (Anscombe, 1973; Matejka and Fitzmaurice, 2017; Yanai and Lercher, 2020). Given the importance of visualization, how do we know which visual methods yield the best perception of information for multivariate data?

Dimension reduction is commonly used with visualization to provide informative low-dimensional summaries of high-dimensional data. In particular, Principal Component Analysis (PCA, Pearson, 1901) remains exceedingly popular. Visualization of PCA is typically in the form static scatterplots of a few of the leading components. Alternatively, a class of dynamic linear projections known as *tours* (Asimov, 1985) was published 16 years prior. Tours also use a scatterplot and biplot display of the data. Instead of a static view of two orthogonal components, they are animated over small changes to the basis. Asimov originally animated between randomly selected bases in the *grand tour*. The *manual tour* (Cook and Buja, 1997) novelly allows for user-control over the basis changes. A selected variable can be rotated to the desired contribution. The permanence of the data points from frame to frame and information held in intermediate interpolated frames or user-control of the basis could plausibly lead to more information perception than a static display. There have been several user studies comparing scatterplots across display dimensionality in dimensionally reduced spaces (Gracia et al., 2016; Wagner Filho et al., 2018). There are also empirical statistics used to describe non-linear reduction and how well and faithfully they embed the data in a lower space (Bertini, Tatú, and Keim, 2011; Liu et al., 2017; Sedlmair, Munzner, and Tory, 2013; Maaten and Hinton, 2008). There is an absence of studies comparing visual techniques.

This paper describes a crowdsourced (prolific.co) user study conducted to assess the efficacy of different visualization methods: PCA as discrete pairs of two components, the grand tour, and the radial tour. *Tours* are animated linear projections over small changes to their bases and described in more detail in Section ?? Cluster data is simulated under several additional experimental factors: location, shape, and dimensionality. We task participants with identifying the variables attributing to the separation between two clusters. We define an accuracy measure for this task. Mixed model regression on this measure finds strong evidence supporting the radial tour has a considerable improvement in accuracy over alternatives.

Knowing which visuals and dimension reduction to use is also important for statistical modeling and their interpretations. Models are becoming increasingly complex involving many interacting, or otherwise non-linear terms cause an opaqueness to their interpretability. Exploratory Artificial Intelligence (XAI, Adadi and Berrada, 2018; Arrieta et al., 2020) is an emerging field that attempts to extend the interpretability of such black-box models by offering techniques to increase their interpretability. Multivariate data visualization is essential for exploring features spaces and communicating interpretations of models (Biecek, 2018; Biecek and Burzykowski, 2021; Wickham, Cook, and Hofmann, 2015).

The paper is structured as follows. Section 3.2 discusses several visualization methods and orthogonal and observation-based visuals before arriving at the three linear dimension reduction techniques compared in the study. Section 3.3 describes the experimental factors, task, and accuracy measure used. The results of the study are discussed in Section 3.4. Conclusions and potential future directions are discussed in Section 3.5. The software used for the study is described in Section 3.6.

3.2 Background

Before discussing PCA, the grand tour, and the radial tour, this section covers orthogonal views and observation-based visuals of the full variable space. Consider data to be a complete matrix of n observations across p variables, $X_{n \times p}$.

3.2.1 Scatterplot matrix

One could consider looking at p histograms or univariate densities. Doing so will miss features in two or more dimensions. A scatterplot matrix (Chambers et al., 1983) is a $p \times p$ matrix with univariate densities on the diagonal and all combinations of pairs of variables in off-diagonal elements. Figure 3.1 shows a scatterplot matrix of the first four components of simulated data. Such displays do not scale well with dimension, quickly becoming dense. Scatterplot matrices also display information in two orthogonal dimensions; features in three dimensions will never be fully resolved.

3.2.2 Parallel coordinates plot

Another common way to display multivariate data is with a parallel coordinates plot (Ocagne, 1885), which shows observations by quantile or normalized values for each variable connected by lines to the quantile value in subsequent variables. Parallel coordinates plot and other observations-based visuals, such as pixel plots or Chernoff faces scale well with dimensions but poorly with observations. These are perhaps best used when there are more variables than observations.

Observations-based visuals have a couple of issues. They are asymmetric across variable ordering, leading to different conclusions or features being focused on due to variable order. Another notable observation-based visual is the graphical channel used to convey information. Munzner suggests that position is the visual channel that is most perceptible to humans (Munzner, 2014). In the case of parallel coordinates plots, the horizontal axes span variables rather than the values of one variable; the loss of a display dimension to be used by most discerning visual channel.

At some point, we will be forced to turn to dimension reduction to scale well. Non-linear transformations bend and distort spaces are not entirely accurate or faithful to the original variable space. In light of this, we preclude non-linear techniques and instead decide on PCA, the grand tour, and the radial tour.

3.2.3 Principal component analysis

PCA is a good baseline of comparison for linear projections because of its frequent and broad use across disciplines. Principal component analysis (Pearson, 1901) defines new components, linear combinations of the original variables, ordered by decreasing variation through the help of eigenvalue matrix decomposition. While the resulting dimensionality is the same size, the benefit comes from the ordered nature of the components. The data can be said to be approximated by the first several components. The exact number is subjectively selected given the variance contained by each component, typically guided using a scree plot (Cattell, 1966). Features with sizable signal regularly appear in the leading components that commonly approximate data. However, this is not always the case, and component spaces should be fully explored to look for signal in components that hold less variation.

3.2.4 Animated linear projections, tours

A data visualization *tour* animates many linear projections over small changes in the projection basis. One of the insightful features of the tour is the object permanence of the data points; one can track the relative changes of observations as the basis moves, as opposed to discretely jumping to an orthogonal view with no intermediate information. Types of tours are distinguished by the selection of their basis paths (Lee et al., 2021; Cook et al., 2008). To contrast with the discrete orientations of PCA, we compare continuous linear projection changes with grand and radial tours.

Grand tours

Target bases are selected randomly in a grand tour (Asimov, 1985). These target bases are then geodesically interpolated for a smooth, continuous path. The grand tour is the first and most widely known tour. The random selection of target bases makes it a general unguided exploratory tool. The grand tour will make a good comparison that has continuity of data points similar to the radial tour but lacks the user control enjoyed by PCA and radial tours.

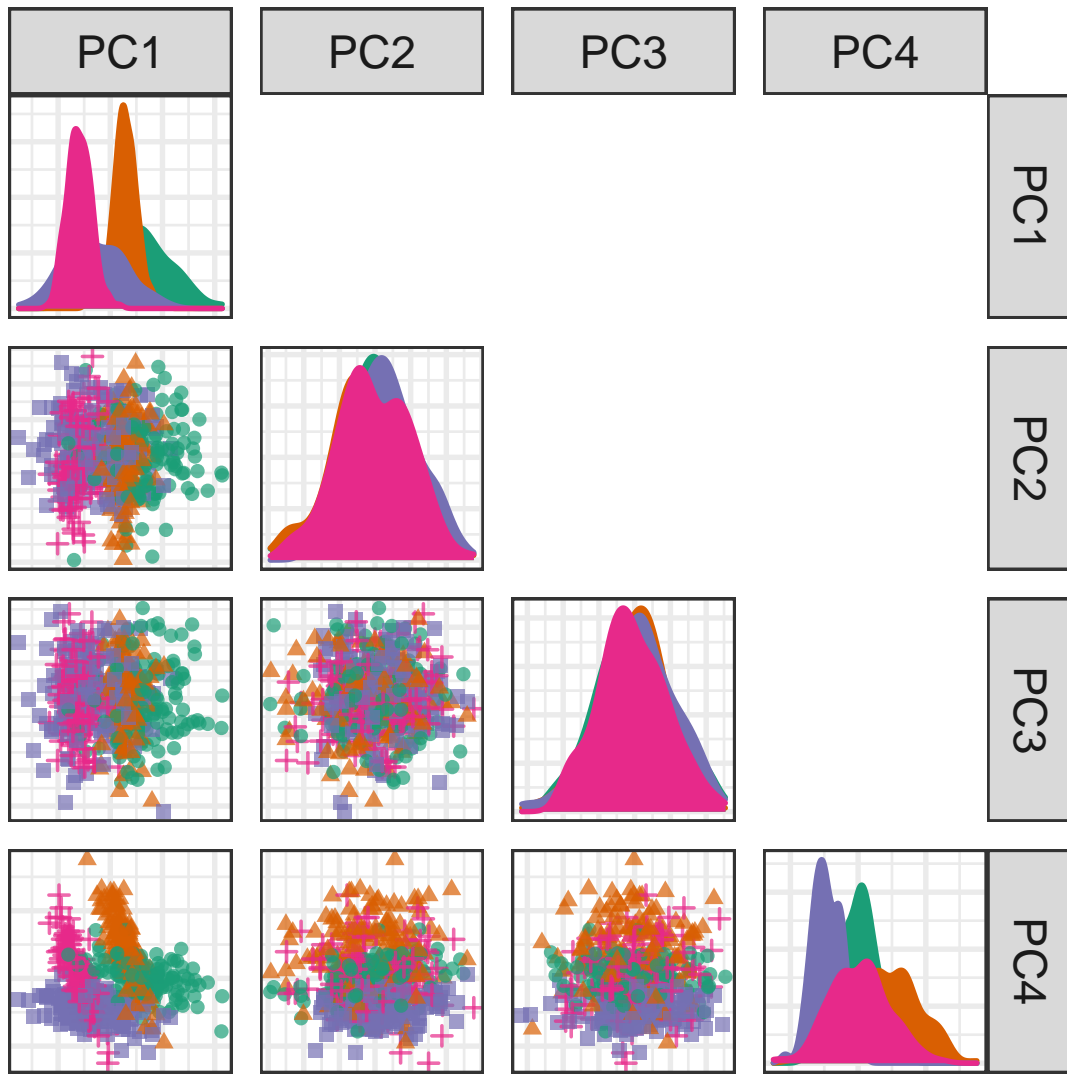


Figure 3.1: Scatterplot matrix of the first four principal components simulated data in six dimensions. An analyst would have to view both PC1 by PC2 and PC1 by PC4 to have a thorough take on which variables attribute to the separation between clusters.

Manual and radial tours

Whether an analyst uses PCA or the grand tour, they cannot influence the basis. They cannot explore the structure identified or change the contribution of the variables. This user-control-steering is a key aspect of *manual* tours that should facilitate testing variable attribution.

The manual tour (Cook and Buja, 1997) defines its basis path by manipulating the basis contribution of a selected variable. A manipulation dimension is appended onto the projection plane, giving a full contribution to the selected variable. The target bases are then chosen to rotate this newly created manipulation space. This manipulation space similarly orthogonally restrained, the data is projected through its interpolated frames and rendered into an animation. When the contribution of one variable changes, the contributions of the other variables must also change, maintaining the orthonormality of the basis and space. A key feature of the manual tour is that it allows users to control the variable contributions to the basis. Such manipulations can be queued in advance or selected in real-time for human-in-the-loop analysis (Karwowski, 2006). Manual navigation is relatively time-consuming due to the vast volume of resulting view space and the abstract method of steering the projection basis. It is advisable first to identify a basis of particular interest and then use the manual tour as a more directed, local exploration tool to explore the sensitivity of a variable's contribution to the feature of interest.

To simplify the task and keep its duration realistic, we consider a variant of the manual tour called a *radial* tour. In a radial tour, the selected variable can change its magnitude of contribution but not its angle; it must move along the direction of its original contribution radius. The radial tour benefits from both continuity of the data alongside grand tours and allows the user to steer via choosing the variable to rotate.

Manual tours have been recently made available in the **R** package **spinifex** (Spyrison and Cook, 2020), which facilitates manual tours (and radial variant). It also provides an interface for a layered composition of tours and exporting to .gif and .mp4 with **gganimate** (Pedersen and Robinson, 2020) or .html widget with **plotly** (Sievert, 2020). It is also compatible with tours made by **tourrr** (Wickham et al., 2011). Now that we have a readily

available means to produce various tours, we want to see how they fare against traditional discrete displays commonly used with PCA.

3.3 User study

An experiment was constructed to assess the performance of the radial tour relative to the grand tour and PCA for interpreting the variable attribution contributing to separation between two clusters. Data were simulated across three experimental factors: cluster shape, location of the cluster separation, and data dimensionality. Participant responses were collected using a web application and crowdsourced through prolific.co, (Palan and Schitter, 2018) an alternative to MTurk.

3.3.1 Objective

PCA will be used as a baseline for comparison as it is the most common linear embedding. The grand tour will act as a secondary control that will help evaluate the benefit of animation without influencing its path. Lastly, the radial tour should perform best as it benefits both from animation and user-control.

Then for some subset of tasks, we expect to find that the radial tour performs most accurately. In the appendix, section 3.9, we also regress on the last response time. Due to the absence of inputs, we expect the grand tour to perform faster than the alternatives since users can focus all of their attention on interpreting the fixed path. Conversely, we are less sure about the accuracy of such limited grand tours as there is no objective function in selecting the bases; it is possible that the random selection of the target bases altogether avoid bases showing cluster separation. However, given that the data dimensionality was modest, it seems plausible that the grand tour coincidentally regularly crossed frames with the correct information for the task.

We measure the accuracy and response time over the support of the discussed experimental factors. The null hypothesis can be stated as:

H_0 : task accuracy does not change across visualization method

H_α : task accuracy does change across visualization method

3.3.2 Experimental factors

In addition to visual factor, we simulate the data across three aspects: 1) The *location* of the difference between clusters by mixing a signal and a noise variable at different ratios, we vary the number of variables and their magnitude of cluster separation, 2) the *shape* of the clusters, to reflect varying distributions of the data, and 3) the *dimension-ality* of the data. Below we describe the levels within each factor, while Figure 3.2 gives a visual representation of the levels.

The *location* of the separation of the clusters is at the heart of the measure. It would be good to test a few varying levels. To test the sensitivity to this, we mix a noise variable with the signal-containing variable. The difference in the clusters is mixed at the following percentages: 0/100% (not mixed), 33/66%, 50/50% (evenly mixed).

In selecting the *shape* of the clusters, we follow the convention given by Scrucca et al. (2016), where 14 variants of model families containing three clusters are defined. The name of the model family is the abbreviation of its respective volume, shape, and orientation of the clusters, the levels of which are either `_E_equal` or `_V_ary`. We use the models EEE, EEV, and EVV. For Instance, in the EEV model, the volume and shape of clusters are constant, while the shape's orientation varies. The latter model is further modified by moving four-fifths of the data out in a “V” or banana-like shape.

Dimension-ality is tested at two modest levels, namely, in four dimensions containing three clusters and six dimensions with four clusters. Such modest dimensionality is required to bound the difficulty and search space to keep the task realistic for crowdsourcing.

3.3.3 Task and evaluation

With our hypothesis formulated and data at hand, let us turn our attention to the task and how to evaluate it. Regardless of the visual method, the elements of the display are

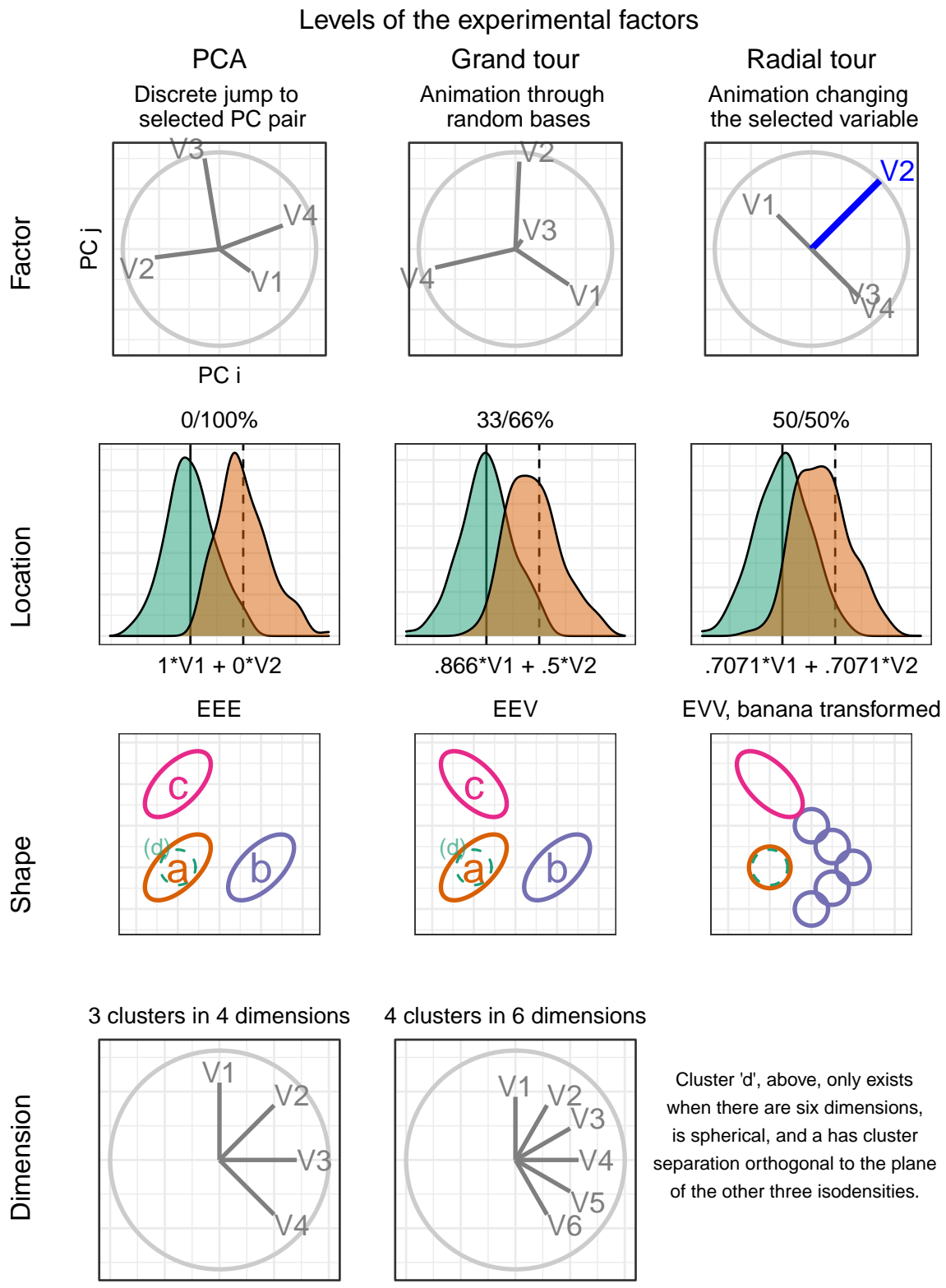


Figure 3.2: Illustration of the experimental factors, the parameter space of the independent variables, the support of our study.

CHAPTER 3. THE BENEFIT OF USER-CONTROLLED RADIAL TOUR FOR UNDERSTANDING VARIABLE CONTRIBUTIONS TO STRUCTURE IN LINEAR PROJECTIONS

held constant, shown as a 2D scatterplot with an axis biplot to its left. Observations were supervised with the cluster level mapped to color and shape.

Participants were asked to ‘check any/all variables that contribute more than average to the cluster separation green circles and orange triangles,’ which was further explained in the explanatory video as ‘mark any and all variable that carries more than their fair share of the weight, or one quarter in the case of four variables’.

The instructions iterated several times in the video was: 1) use the input controls to find a frame that contains separation between the clusters of green circles and orange triangles, 2) look at the orientation of the variable contributions in the gray circle (biplot axes orientation), and 3) select all variables that contribute more than uniformed distributed cluster separation in the scatterplot. Independent with experimental level, participants were limited to 60 seconds for each evaluation of this task. This restriction did not impact many participants as the 25th, 50th, 75th quantiles of the response time were about 7, 21, and 30 seconds respectively.

The evaluation measure of this task was designed with a few of features in mind: 1) the sum of squares of the individual variable weights should be one, 2) symmetric about zero, that is, without preference to under- or over-guessing 3) heavier than linear weight with increasing distance from a uniform height. With these in mind, we define the following measure for evaluating the task.

Let a data $\mathbf{X}_{n \times p}$ be a simulation containing clusters of observations of different distributions. Where n is the number of observations, p is the number of variables, and k indicates the number of the cluster an observation belongs. Cluster membership is exclusive; an observation cannot belong to more than one cluster.

We define weights, W as a vector explaining the variable-wise difference between two clusters. Namely, the difference of each variable between clusters, as a proportion of the total difference, less $1/p$, the amount of difference each variable would hold if it were uniformly distributed. Participant responses are a logical value for each variable - whether or not the participant thinks each variable separates the two clusters more than uniformly distributed separation. Then Y is a vector of variable accuracy.

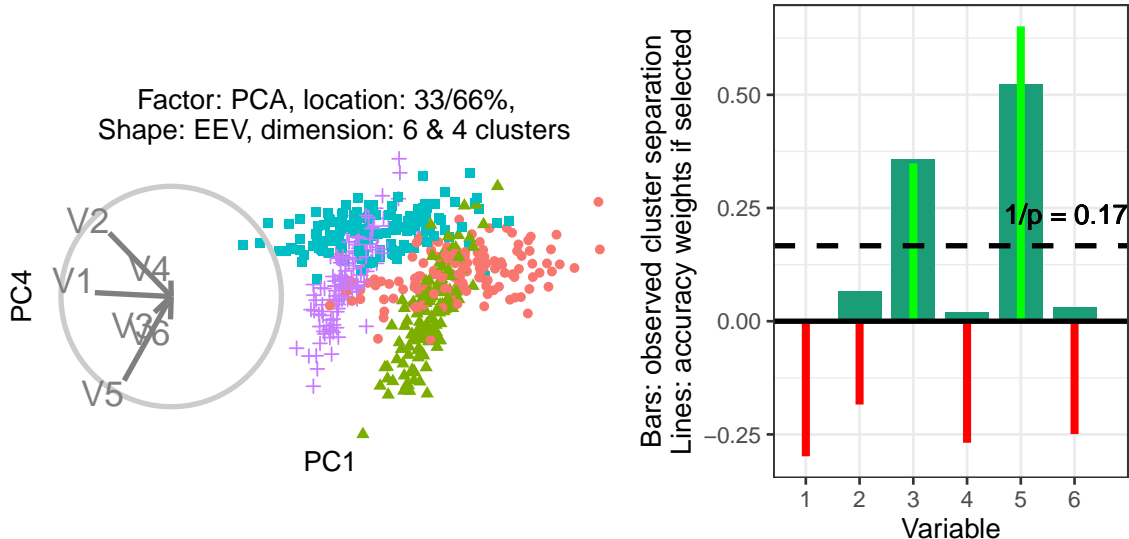


Figure 3.3: (L), PCA biplot of the components showing the most cluster separation with (R) illustration of the magnitude of cluster separation is for each variable (bars) and the weight of the variable accuracy if selected (red/green lines). The horizontal dashed line is $1/p$, the amount of separation each variable would have if evenly distributed. The weights equal the signed square of the difference between each variable value and the dashed line.

$$W_i = \frac{(\bar{X}_{i=1,k=1} - \bar{X}_{1,2}, \dots, (\bar{X}_{p,1} - \bar{X}_{p,2})}{\sum_{i=1}^p (|\bar{X}_{i,k=1} - \bar{X}_{i,2}|)} - \frac{1}{p}$$

$$\text{Accuracy, } Y = \sum_{i=1}^p I(r_i) \cdot \text{sign}(w_i) \cdot \begin{cases} \frac{w_+^2}{\sum w_+^2} & \left| w_+ \text{ the positive elements of } w \right. \\ \frac{w_-^2}{\sum w_-^2} & \left| w_- \text{ the negative elements of } w \right. \end{cases}$$

Where $I(r_i)$ is the indicator function on the response for variable i .

3.3.4 Visual design standardization

The factors are tested within-participant, with each visual being evaluated twice by each participant. The order that experimental factors are experienced is controlled with the assignment, as illustrated in Figure 3.4. Below we cover the visual design standardization and the input and display within each factor.

CHAPTER 3. THE BENEFIT OF USER-CONTROLLED RADIAL TOUR FOR UNDERSTANDING VARIABLE CONTRIBUTIONS TO STRUCTURE IN LINEAR PROJECTIONS

The visualization methods were standardized wherever possible. Data were displayed as 2D scatterplots with biplots (Gabriel, 1971), a visual with variable contributions inscribed on a unit circle. All aesthetic values (colors, shapes, sizes, absence of legend, and axis titles) were constant. Variable contributions were always shown left of the scatterplot embeddings with their aesthetic values consistent. What did vary between factors were their inputs.

PCA inputs allowed users to select between the top four principal components for both the x- and y-axis regardless of the data dimensionality (four or six). Data was simulated to have cluster separation within the 2nd to 4th components, ideally not simple enough to be entirely observed in PC1 by PC2. But not burying signal in 5th and 6th components (not selectable in PCA input) in the interest of simplicity and time. There was no user input for the grand tour; users were instead shown a 15-second animation of the same randomly selected path. Participants could view the same clip up to four times within the time limit. Radial tours were also displayed at five frames per second with a step size of 0.1 radians between interpolated frames. Users were able to swap between variables. The display would change the start of radially increasing the contribution of the selected variable until it was full, zeroed, and then back to its initial contribution. The complete animation of any variable takes about 20 seconds and is almost entirely in the projection frame at around six seconds. The starting basis was initialized to a half-clock design, where the variables were evenly distributed in half of the circle. This design was created to be variable agnostic while maximizing the independence of the variables.

3.3.5 Data simulation

Each dimension is originally distributed as $\mathcal{N}(0, 1)$ | covariance Σ , a function of the shape factor. Clusters were originally separated by a distance of two before location mixing. Signal variables had a correlation of 0.9 when they had equal orientation and -0.9 when their orientations vary. Noise variables were restricted to zero correlation. Each cluster is simulated with 140 observations and is offset in a variable that did not distinguish previous variables.

Clusters of the EVV shape are transformed to the banana-chevron shape (illustrated in figure 3.2, shape row). Then location mixing is applied by post-multiplying a (2x2) rotation

CHAPTER 3. THE BENEFIT OF USER-CONTROLLED RADIAL TOUR FOR UNDERSTANDING VARIABLE CONTRIBUTIONS TO STRUCTURE IN LINEAR PROJECTIONS

matrix to the signal variable and a noise variable for the clusters in question. All variables are then standardized by standard deviation. The rows and columns are then shuffled randomly. The observation's cluster and order of shuffling are attached to the data and saved.

Each of these replications is then iterated with each level of the factor. For PCA, every pair of the top four principal components and saved as 12 plots. We first save two basis paths of differing dimensions for the grand tour before each replication is projected through the common basis path. Each simulation's variable order was previously shuffled effectually randomizing cluster separation shown, while mitigating bias from fringe selection of target bases. The resulting animations were saved as .gif files. The radial tour starts at either the four or six variable “half-clock” basis, where each variable has a uniform contribution in the right half and no variable contributing in the opposite direction (to minimize the dependence between variable contributions), a radial tour is then produced for each variable and saved as a .gif.

3.3.6 Randomized factor assignment

Now, with simulation and their artifacts in hand, we explain how the experimental factors are assigned and illustrate how this is experienced from a participant's perspective.

We section the study into three periods. Each period is linked to a randomized level of factor visualization and the location. The order of dimension and shape are of secondary interest and are held constant in increasing order of difficulty; four then six dimensions and EEE, EEV, then EVV-banana, respectively.

Each period starts with an untimed training task at the simplest remaining experimental levels; location = 0/100%, shape = EEE, and four dimensions with three clusters. This serves to introduce and familiarize participants with input and visual differences. After the training, the participant is evaluated on two tasks with the same factor and location level across the increasing difficulty of dimension and shape. The plot was removed after 60 seconds, though this limit was rarely reached by participants.

CHAPTER 3. THE BENEFIT OF USER-CONTROLLED RADIAL TOUR FOR UNDERSTANDING VARIABLE CONTRIBUTIONS TO STRUCTURE IN LINEAR PROJECTIONS

Consider a new participant, the 63rd participant,

- 1) Set the factor order:

$$1 + (63 - 1) \bmod 6 = \\ \text{permutation 4;} \\ \text{grand, PCA, \& radial}$$

- 2) Set location order:

$$1 + \text{floor}((63 - 1) / 6) \bmod 36 = \\ \text{permutation 3; 33/67, 50/50,} \\ \& 0/100 \% \text{ noise/signal mix}$$

Fixed factors:

- 3) Variance-covariance shape increments with each period: EEE, EEV, EVV-banana
4) Data dimension is fixed within each period: 4 then 6

factor order permutation	Period 1			Period 2			Period 3		
	1	2	3	1	2	3	1	2	3
1	P	G	R		1	2	3		
2	P	R	G		2	1	3	2	
3	G	R	P		3	2	3	1	
4	G	P	R		4	2	1	3	
5	R	P	G		5	3	1	2	
6	R	P	G		6	3	2	1	

Increment through all permutations of factor, before incrementing 1 permutation of location

Period	Evaluation order	Factor ¹	Location ²	Shape ³	Dimensions ⁴
1	Train 1	Grand	0/100	EEE	4 (3cl)
1	1	Grand	33/67	EEE	4 (3cl)
1	2	Grand	33/67	EEE	6 (4cl)
2	Train 2	PCA	0/110	EEE	4 (3cl)
2	3	PCA	50/50	EV	4 (3cl)
2	4	PCA	50/50	EV	6 (4cl)
3	Train 3	Radial	0/100	EEE	4 (3cl)
3	5	Radial	0/100	Ban	4 (3cl)
3	6	Radial	0/100	Ban	6 (4cl)

Figure 3.4: Illustration of how a hypothetical participant 63 is assigned experimental factors. Each of the 6 factor order permutations is exhausted before iterating to the next permutation of location order.

The order of the factor and location levels is randomized with a nested Latin square where all levels of the visual factor are exhausted before advancing to the next level of location. That means we need $3!^2 = 36$ participants to evaluate all permutations of the experimental factors once. This randomization controls for potential learning effects the participant may receive. Figure 3.4 illustrates how an arbitrary participant experiences the experimental factors.

Through pilot studies sampled by convenience (information technology and statistics Ph.D. students attending Monash University), we predict that we need three full evaluations to properly power our study; we set out to crowdsource $N = 3 \cdot 3!^2 = 108$ participants.

3.3.7 Participants

We recruited $N = 108$ participants via prolific.co (Palan and Schitter, 2018). We filtered participants based on their claimed education requiring that they have completed at least an undergraduate degree (some 58,700 of the 150,400 users at the time); we apply this filter under the premise that linear projections and biplot displays will not be regularly used for consumption by general audiences. There is also the implicit filter that Prolific

51

CHAPTER 3. THE BENEFIT OF USER-CONTROLLED RADIAL TOUR FOR UNDERSTANDING VARIABLE CONTRIBUTIONS TO STRUCTURE IN LINEAR PROJECTIONS

participants must be at least 18 years of age and implicit biases of timezone, location, and language. Participants were compensated for their time at £7.50 per hour, whereas the mean duration of the survey was about 16 minutes. We cannot preclude previous knowledge or experience with the factors but validate this assumption in the follow-up survey asking about familiarity with the factors. The appendix contains a heatmap distribution of age and education paneled across preferred pronouns of the participants that completed the survey, who are relatively young, well educated, and slightly more likely to identify as males.

3.3.8 Data collection

Data were recorded by a **shiny** application and written to a Google Sheet after each third of the study. Especially at the start of the study, participants experienced adverse network conditions due to the volume of participants hitting the application with modest allocated resources. In addition to this, API read/write limitations further hindered data collection. To mitigate this, we throttled the number of participants and over-collect survey trials until we received our target three evaluations of all permutation levels.

The processing steps were minimal. First, we format to an analysis-ready form, decoding values to a more human-readable state, and add a flag indicating whether the survey had complete data. We filter to only the latest three complete studies of each experimental factor, which should have experienced the most minor adverse network conditions. The bulk of the studies removed were partial data and a few over-sampled permutations. This brings us to the 108 studies described in the paper, from which models and aggregation tables were built. The post-study surveys were similarly decoded to human-readable format and then filtered to include only those 84 associated with the final 108 studies.

The code, response files, their analyses, and the study application are publicly available at on GitHub; https://github.com/nspyrison/spinifex_study.

3.4 Results

To recap, the primary response variable is task accuracy, as defined in section 3.3.3. The parallel analysis of the log response time is provided in the appendix. We have two primary data sets; the user study evaluations and the post-study survey. The former is the 108 participants with the explanatory variables: visual factor, location of the cluster separation signal, the shape of variance-covariance matrix, and the dimensionality of the data. Experimental factors and randomization were discussed in section ???. The survey was completed by 84 of these 108 people. It collected demographic information (preferred pronoun, age, and education), and subjective measures for each factor (preference, familiarity, ease of use, and confidence).

Below we build a battery of mixed regression models to explore the degree of the evidence and the size of the effects from the experimental factors. Then, we use likert plots and rank-sum tests to compare the subjective measures between the visual factors.

3.4.1 Accuracy regression

To more thoroughly examine explanatory variables, we regress against accuracy. All models have a random effect term on the participant and the simulation. These terms explain the error that can be attributed to the effect of the individual participant and variation due to the random sampling data.

In building a set of models to test, we include all single term models with all independent terms. We also include an interaction term for factor and location, allowing for the slope of each location to change across each level of the factor. For comparison, an overly complex model with all interaction terms is included. The matrices for models with more than a two terms is rank deficient; there is not enough varying information in the data to explain all interacting terms.

CHAPTER 3. THE BENEFIT OF USER-CONTROLLED RADIAL TOUR FOR
UNDERSTANDING VARIABLE CONTRIBUTIONS TO STRUCTURE IN LINEAR
PROJECTIONS

Table 3.1: Model performance of random effect models regressing accuracy. Each model includes a random effect term of the participant explaining the individual's influence on accuracy. Complex models perform better in terms of R^2 and RMSE, yet AIC and BIC penalizes their large number of fixed effects in favor of the much simpler model containing only the visual factor. Conditional R^2 includes the random effects, while marginal does not.

Fixed effects	No. levels	No. terms	AIC	BIC	R2 cond.	R2 marg.	RMSE
a	1	3	1000	1027	0.180	0.022	0.462
a+b+c+d	4	8	1026	1075	0.187	0.030	0.460
a*b+c+d	5	12	1036	1103	0.198	0.043	0.457
a*b*c+d	8	28	1069	1207	0.238	0.080	0.447
a*b*c*d	15	54	1125	1380	0.282	0.111	0.438

Fixed effects Full model

$$\begin{aligned}
 \alpha & \quad \hat{Y} = \mu + \alpha_i + \mathbf{Z} + \mathbf{W} + \epsilon \\
 \alpha + \beta + \gamma + \delta & \quad \hat{Y} = \mu + \alpha_i + \beta_j + \gamma_k + \delta_l + \mathbf{Z} + \mathbf{W} + \epsilon \\
 \alpha \cdot \beta + \gamma + \delta & \quad \hat{Y} = \mu + \alpha_i \cdot \beta_j + \gamma_k + \delta_l + \mathbf{Z} + \mathbf{W} + \epsilon \\
 \alpha \cdot \beta \cdot \gamma + \delta & \quad \hat{Y} = \mu + \alpha_i \cdot \beta_j \cdot \gamma_k + \delta_l + \mathbf{Z} + \mathbf{W} + \epsilon \\
 \alpha \cdot \beta \cdot \gamma \cdot \delta & \quad \hat{Y} = \mu + \alpha_i \cdot \beta_j \cdot \gamma_k \cdot \delta_l + \mathbf{Z} + \mathbf{W} + \epsilon
 \end{aligned}$$

where α_i , fixed term for factor | $i \in (\text{pca, grand, radial})$

β_j , fixed term for location | $j \in (0/100\%, 33/66\%, 50/50\%)$ % noise/signal mixing

γ_k , fixed term for shape | $k \in (\text{EEE, EEV, EVV banana})$ model shapes

δ_l , fixed term for dimension | $l \in (4 \text{ variables \& 3 cluster, 6 variables \& 4 clusters})$

μ is the intercept of the model including the mean of random effect

$\mathbf{Z} \sim \mathcal{N}(0, \tau)$, the error of the random effect of participant

$\mathbf{W} \sim \mathcal{N}(0, v)$, the error of the random effect of simulation

$\epsilon \sim \mathcal{N}(0, \sigma)$, the remaining error in the model

We also want to visually explore the conditional variables in the model. Figure 3.5 explores violin plots of accuracy by factor while faceting on the location (vertical) and shape (horizontal). Use of the radial visual, on average, increases the accuracy, and especially so when the location of signal mixing is not 33/66%.

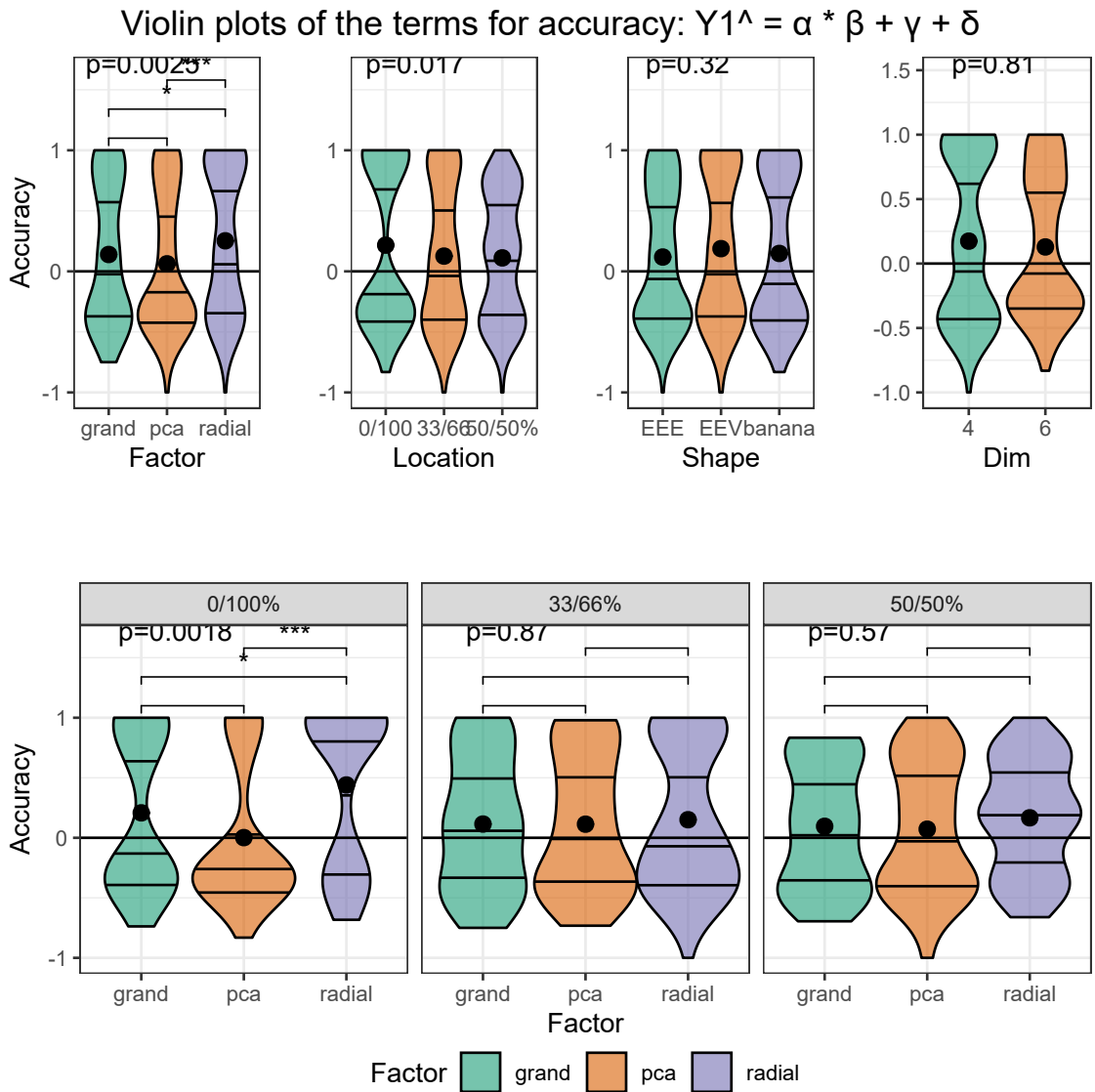


Figure 3.5: Violin plots of terms of the model $\hat{Y} = \alpha \cdot \beta + \gamma + \delta$. Overlaid with global significance from the Kruskal-Wallis test and pairwise significance from the Wilcoxon test, both are non-parametric, ranked-sum tests suitable for handling discrete data. Participants are more confident and find the radial tour easier to use than the grand tour. Participants claim low familiarity, as we expect from crowdsourced participants. Radial is more preferred compared with either alternative for this task.

Table 3.2: The task accuracy model coefficients for $\hat{Y} = \alpha \cdot \beta + \gamma + \delta$, with factor = pca, location = 0/100%, and shape = EEE held as baselines. Factor being radial is the fixed term with the strongest evidence supporting the hypothesis. When crossing the visual factor there is some evidence suggesting radial performs worse with 33/66% mixing. The model fit is based on the 648 evaluations by the 108 participants.

	Estimate	Std. Error	df	t value	Pr(> t)
(Intercept)	0.03	0.08	44.2	0.44	0.66
factor					
Factorpca	-0.15	0.09	622.4	-1.74	0.08
Factorradial	0.22	0.09	618.6	2.46	0.01 *
fixed effects					
Location33/66%	0.10	0.09	84.9	1.09	0.28
Location50/50%	0.05	0.09	83.0	0.58	0.56
ShapeEEV	0.04	0.06	11.5	0.79	0.44
Shapebanana	-0.03	0.06	11.5	-0.48	0.64
Dim6	-0.06	0.05	11.5	-1.39	0.19
interactions					
Factorpca:Location33/66%	0.06	0.13	587.3	0.49	0.63
Factorradial:Location33/66%	-0.28	0.13	577.6	-2.14	0.03 *
Factorpca:Location50/50%	0.09	0.13	589.6	0.68	0.50
Factorradial:Location50/50%	-0.10	0.13	588.0	-0.77	0.44

3.4.2 Subjective measures

The 84 evaluations of the post-study survey also collect four subjective measures for each factor. Figure ?? shows the Likert plots, or stacked percentage bar plots, alongside violin plots with the same non-parametric, ranked sum tests previously used. Participants preferred to use radial for this task. Participants were also more confident of their answers and found radial tours easier than grand tours. All factors have reportedly low familiarity, as expected from crowdsourced participants.

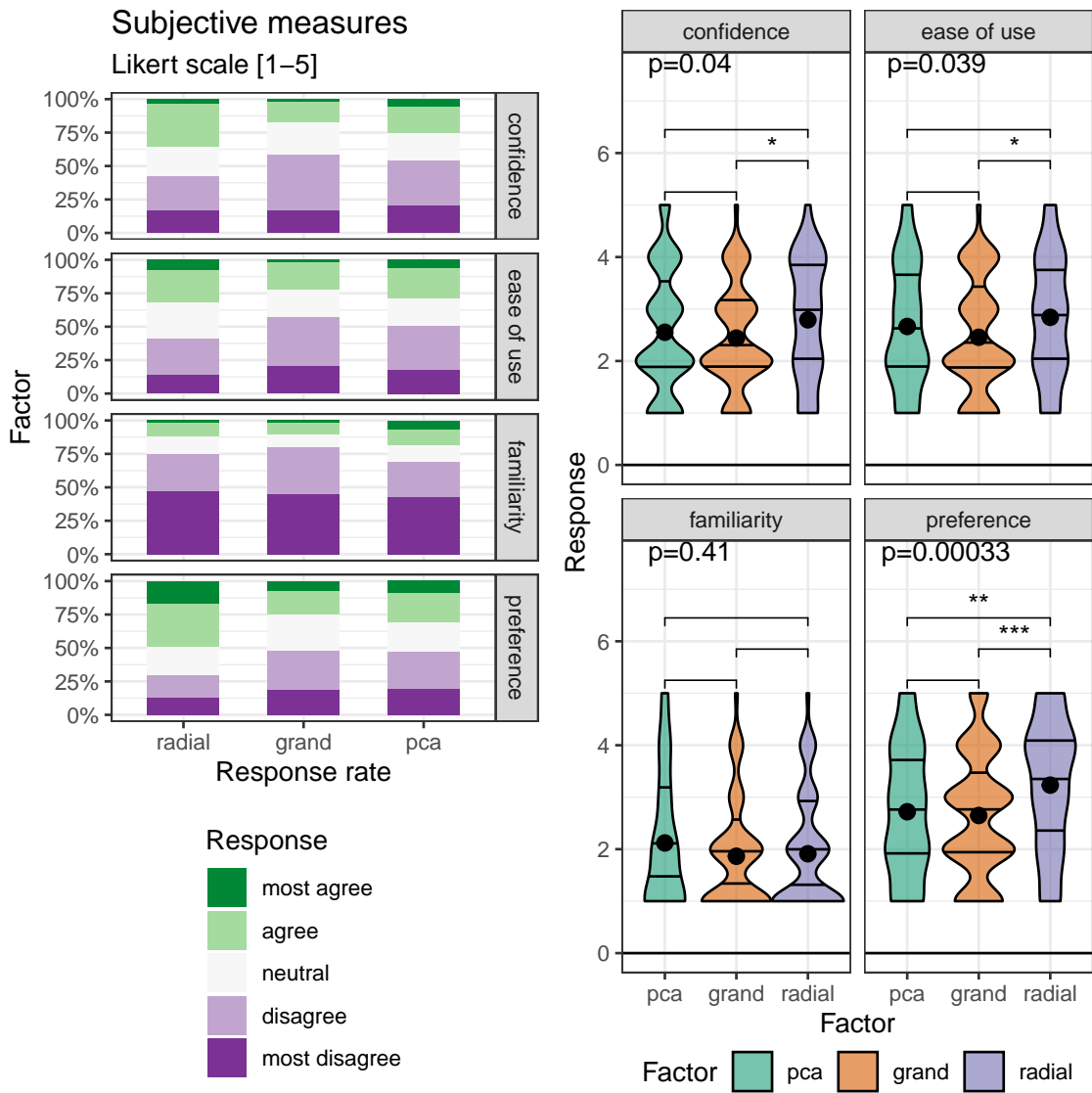


Figure 3.6: The subjective measures of the 84 responses of the post-study survey, five discrete Likert scale levels of agreement (L) Likert plots (stacked percent bar plots) with (R) violin plots of the same measures. Violin plots are overlaid with global significance from the Kruskal-Wallis test, and pairwise significance from the Wilcoxon test, both are non-parametric, ranked sum tests.

3.5 Conclusion

Data visualization is an integral part of EDA. Yet through exploration of data in high dimensions become difficult. Previous methods offer no means for an analyst to impact the projection basis. The manual tour provides a mechanism for changing the contribution of a selected variable to the basis. Giving analysts such control should facilitate the exploration of variable-level sensitivity to the identified structure. We find strong evidence that using the radial tour improves the accuracy relative to PCA or the grand tour on the supervised cluster task assigning variable attribution to the separation of the two clusters.

This paper discussed a with-in participant user study ($n = 108$) comparing the efficacy of three linear projection techniques. The participants performed a supervised cluster task, explicitly identifying which variables contribute to separating two target clusters. This was evaluated evenly over four experimental factors. In summary, we find strong evidence that using the radial tour leads to a sizable accuracy increase. In the appendix we find evidence for a small change in response time, with PCA being fastest, then the grand tour followed by the radial tour. The effect sizes on accuracy are large relative to the change from the other experimental factors, though smaller than the random effect of the participant. The radial tour was subjectively preferred, leading to more confidence in answers, and increased ease of use than the alternatives.

There are several ways that this study could be extended. In addition to expanding the support of the experimental factors, more exciting directions include: changing the type of the task, visualizations used, and experience level of the target population. It is difficult to achieve good coverage given the number of possible permutations. Keep in mind the traffic volume and low effort of responses from participants when crowdsourcing.

3.6 Accompanying tool: radial tour application

We have produced an application to illustrate the radial tour to accompany this study. The **R** package, **spinifex**, (Spyrison and Cook, 2020) is free, open-source and now contains a **shiny** (Chang et al., 2020) application that allows users to apply various preprocessing tasks and interactively explore their data via interactive radial tour. Example datasets are

CHAPTER 3. THE BENEFIT OF USER-CONTROLLED RADIAL TOUR FOR UNDERSTANDING VARIABLE CONTRIBUTIONS TO STRUCTURE IN LINEAR PROJECTIONS

provided with the ability to upload data. The .html widget produced is a more interactive variant relative to the one used in the user study. Screen captures and more details are provided in the appendix. Run the following **R** code will run the application locally.

```
## Download:  
install.packages("spinifex", dependencies = TRUE)  
## Run interactive app demonstrating the radial tour:  
spinifex::run_app()
```

3.7 Acknowledgments

This research was supported by an Australian Government Research Training Program (RTP) scholarship. This article was created in **R** (R Core Team, 2020) and **rmarkdown** (Xie, Allaire, and Grolemund, 2018). Visuals were prepared with **spinifex**. All packages used are available from the Comprehensive R Archive Network **CRAN**. The source files for this article, application, data, and analysis can be found on **GitHub**. The source code for the **spinifex** package and accompanying shiny application can be found **here**. We thank Jieyang Chong for his help in proofreading this article.

3.8 References

00

3.9 Appendix

Survey participant demographics

The target population is relatively well-educated people, as linear projections may prove difficult for generalized consumption. Hence we restrict Prolific.co participants to those with an undergraduate degree (58,700 of the 150,400 users at the study time). From this cohort, 108 performed a complete study. Of these participants, 84 submitted the post-study survey, represented in the following heatmap. All participants were compensated for their time at £7.50 per hour, with a mean time of about 16 minutes.

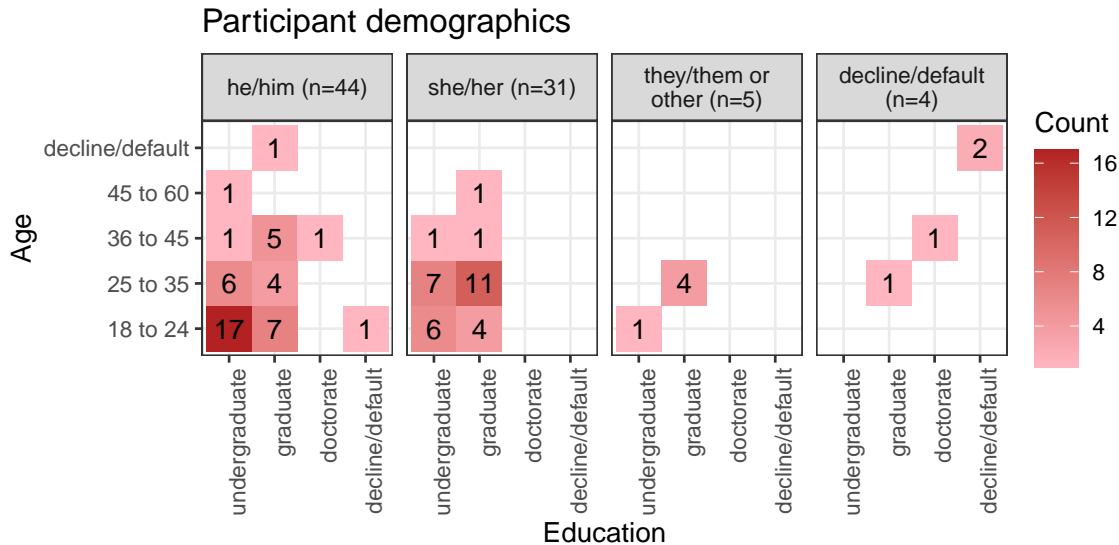


Figure 3.7: Heatmaps of survey participant demographics; counts of age group by completed education as faceted across preferred pronoun. Our sample tended to be between 18 and 35 years of age with an undergraduate or graduate degree.

Table 3.3: Model performance regressing on log response time [seconds], \widehat{Y}_2 random effect models, where each includes random effect terms for participants and simulations. We see the same trade-off where AIC/BIC prefer the simplest factor model, while R^2 and RMSE is the largest in the full multiplicative model. We again select the model $\alpha \cdot \beta + \gamma + \delta$ to explore further as it has relatively high marginal R^2 while having much less complexity than the complete interaction model. Conditional R^2 includes the random effects, while marginal does not.

Fixed effects	No. levels	No. terms	AIC	BIC	R2 cond.	R2 marg.	RMSE
a	1	3	1000	1027	0.180	0.022	0.462
a+b+c+d	4	8	1026	1075	0.187	0.030	0.460
a*b+c+d	5	12	1036	1103	0.198	0.043	0.457
a*b*c+d	8	28	1069	1207	0.238	0.080	0.447
a*b*c*d	15	54	1125	1380	0.282	0.111	0.438

3.9.1 Response time regression

As a secondary explanatory variable, we also want to look at time. First, we take the log transformation of time as it is right-skewed. We repeat the same modeling procedure: 1) Compare the performance of a battery of all additive and multiplicative models. 2) Select the model with the same effect terms, $\alpha \cdot \beta + \gamma + \delta$, and examine its coefficients.

CHAPTER 3. THE BENEFIT OF USER-CONTROLLED RADIAL TOUR FOR
UNDERSTANDING VARIABLE CONTRIBUTIONS TO STRUCTURE IN LINEAR
PROJECTIONS

Table 3.4: Model coefficients for log response time [seconds] $\widehat{Y}_2 = \alpha \cdot \beta + \gamma + \delta$, with factor = PCA, location = 0/100%, and shape = EEE held as baselines. Location = 50/50% is the fixed term with the strongest evidence and takes less time. In contrast, the interaction term location = 50/50%:shape = EEV has the most evidence and takes much longer on average.

	Estimate	Std. Error	df	t value	Pr(> t)	
(Intercept)	2.48	0.14	42.8	17.41	0.00	***
Factor						
Factorpca	0.23	0.12	567.6	1.97	0.05	*
Factorradial	0.39	0.12	571.9	3.29	0.00	**
Fixed effects						
Location33/66%	0.29	0.14	42.0	2.06	0.05	*
Location50/50%	0.07	0.14	40.5	0.54	0.59	
ShapeEEV	-0.15	0.09	8.3	-1.61	0.14	
Shapebanana	-0.13	0.09	8.3	-1.42	0.19	
Dim6	0.14	0.08	8.3	1.90	0.09	
Interactions						
Factorpca:Location33/66%	-0.24	0.18	580.9	-1.34	0.18	
Factorradial:Location33/66%	-0.48	0.18	583.1	-2.63	0.01	**
Factorpca:Location50/50%	-0.12	0.18	578.6	-0.69	0.49	
Factorradial:Location50/50%	-0.08	0.18	580.9	-0.43	0.67	

Random effect ranges

Residual plots have no noticeable non-linear trends and contain striped patterns as an artifact from regressing on discrete variables. Figure 3.8 illustrates (T) the effect size of the random terms participant and simulation, or more accurately, the 95% CI from Gelman simulation of their posterior distribution. The effect size of the participant is much larger than simulation. The most extreme participants are statistically significant at $\alpha = .95$, while none of the simulation effects significantly deviate from the null of having no effect size on the marks. In comparison, (B) 95% confidence intervals participation and simulation mean accuracy, respectively.

Similarly, figure 3.9 shows the Gelman simulations and marginal effects of the simulation and participants for Y_2 , the same model regressing on log response time.

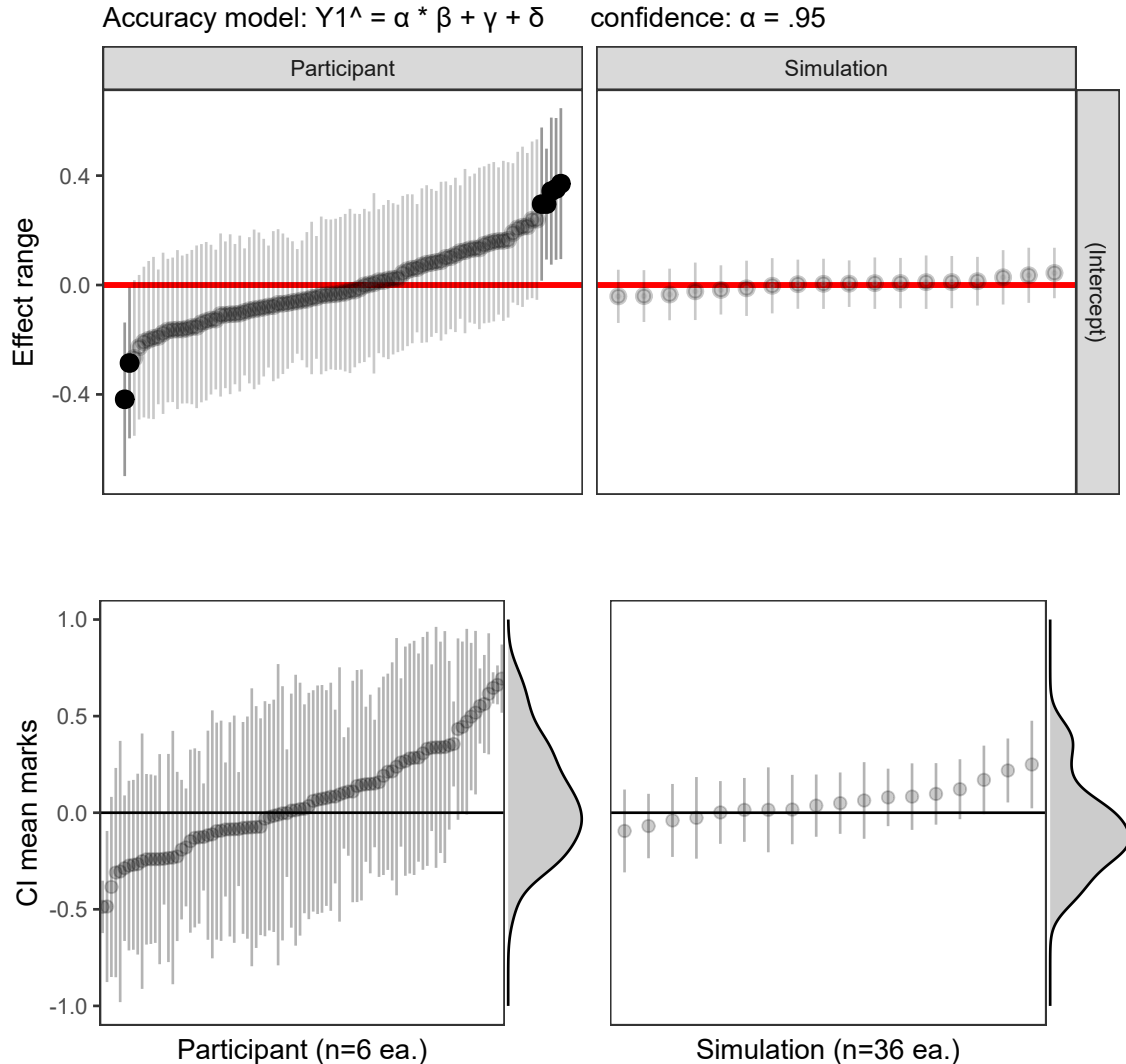


Figure 3.8: Accuracy model: (T) Estimated effect ranges of the random effect terms participant and data simulation of the accuracy model, $\widehat{Y}_1 = \alpha \cdot \beta + \gamma + \delta$. Confidence intervals are created with Gelman simulation on the effect posterior distributions. The effect size of the participant is relatively large, with several significant extrema. None of the simulations deviate significantly. (B) The ordered distributions of the CI of mean marks follow the same general pattern and give the additional context of how much variation is in the data, an upper limit to the effect range. The effect ranges capture about two-thirds of the range of the data without the model. All intervals for $\alpha = .95$ confidence.

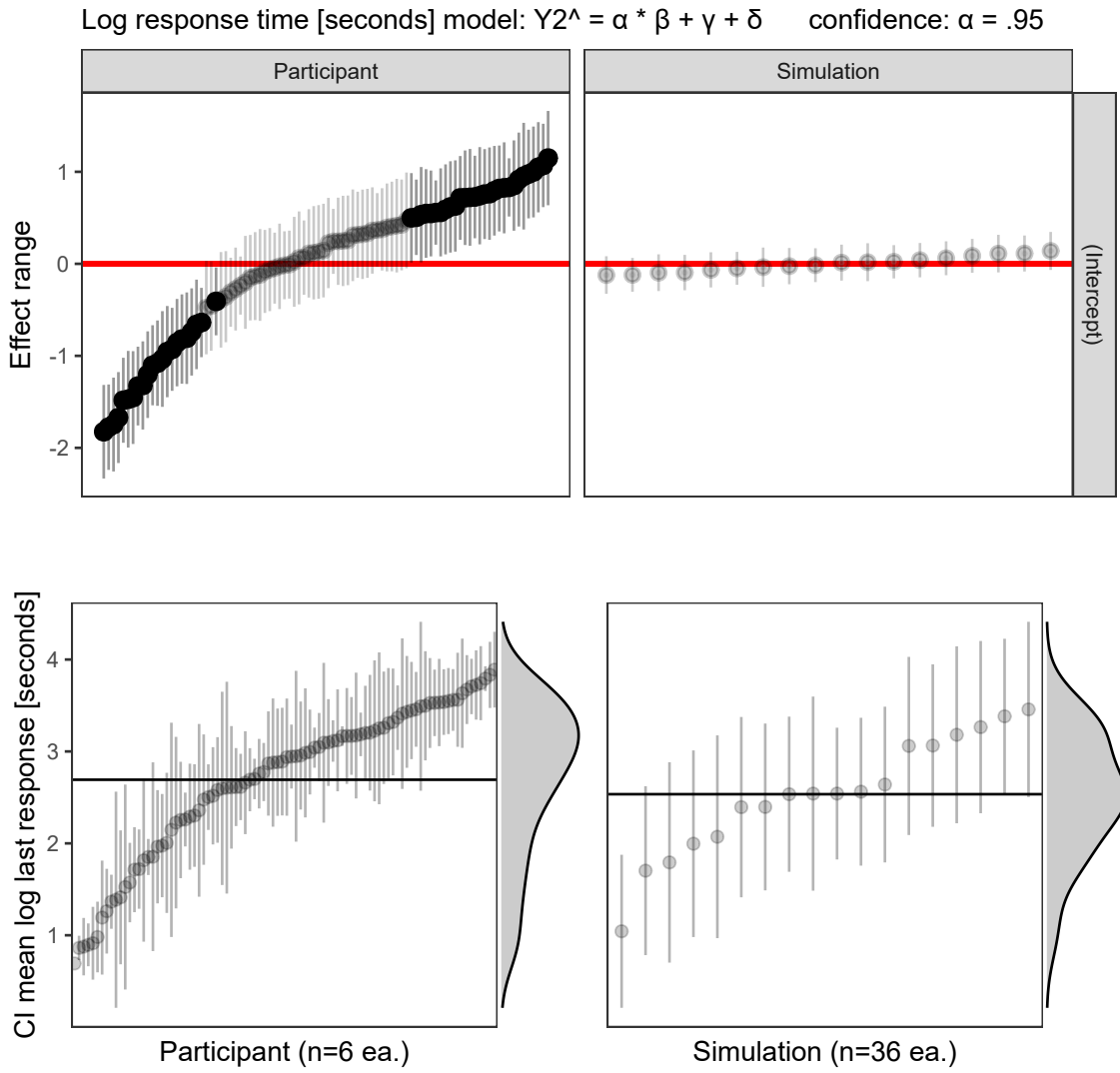
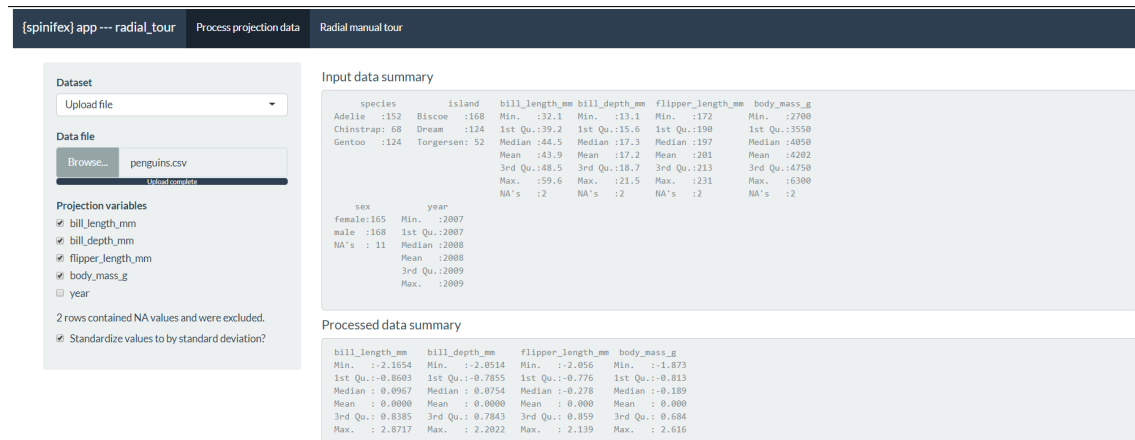


Figure 3.9: Log response time model: (T) The effect ranges of Gelman resimulation on posterior distributions for the time model, $\tilde{Y}_2 = \alpha \cdot \beta + \gamma + \delta$. These show the magnitude and distributions of particular participants and simulations. Simulation has a relatively small effect on response time. (B) Confidence intervals for mean log time by participant and simulation. The marginal density shows that the response times are left-skewed after log transformation. Interpreting back to linear time there is quite the spread of response times: $e^1 = 2.7$, $e^{2.75} = 15.6$, $e^{3.75} = 42.5$ seconds. Of the simulations on the right, the bottom has a large variation in response time, relative to the effect ranges which means that the variation is explained in the terms of the model and not by the simulation itself.

CHAPTER 3. THE BENEFIT OF USER-CONTROLLED RADIAL TOUR FOR UNDERSTANDING VARIABLE CONTRIBUTIONS TO STRUCTURE IN LINEAR PROJECTIONS



radial_tour app, ---{spinifex} ver. 0.3.0 --- 2021-07-01

Figure 3.10: *Process data tab, interactively loads or select data, check which variables to project, and optionally scale columns by standard deviation.*

Radial tour application details

Below we describe the **shiny** app available in the **spinifex** package which runs locally. It streamlines creating and interacting with radial tours more interactive than the application used in the user study.

In the initial tab, users upload their own (.csv, .rds, or .rda) data or select from predefined data sets. The numeric columns appear as a list of variables to include in the projection. Below that, a line displays whether or not missing rows were removed. Scaling by standard deviation is included by default, as this is a common transformation used to explore linear projections of spaces. Summaries of the raw data and processed numeric data are displayed to illustrate how the data was read and its transformation.

The second tab contains interaction for selecting the manipulation variable and non-numeric columns can be used to change the color and shape of the data points in the projection. The radial tour is created in real-time, animated as an interactive **plotly** .html widget. The application offers users a fast, intuitive introduction elucidating what the radial tour does and some of the features offered.

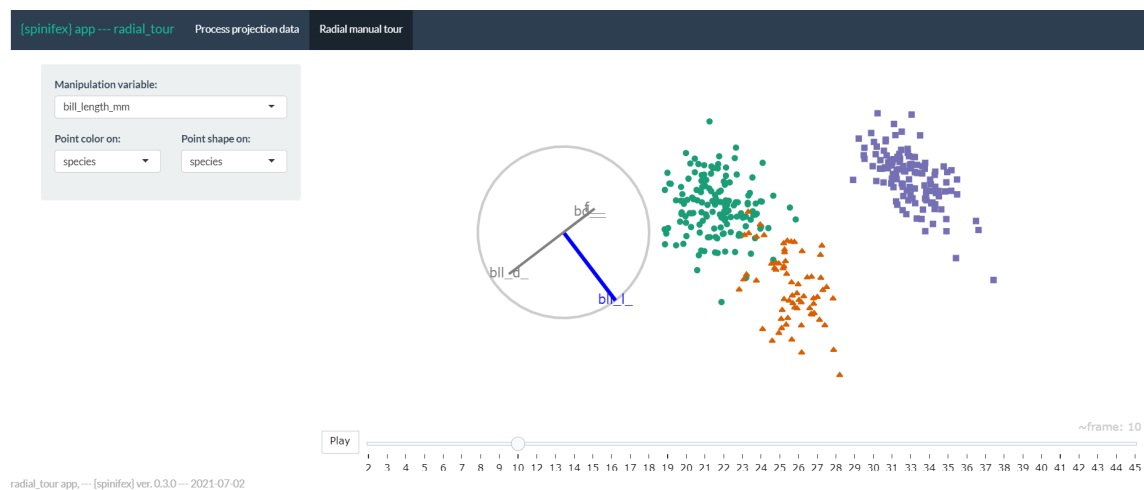


Figure 3.11: Radial tour tab, interactively create radial tours, changing the manipulation variable, and color or shape of the resulting manual tour. Here, the palmer penguins data is being explored, bill length was selected to manipulate as it is the only variable separating the green cluster from the orange. By mapping shape to island of observation, we also notice that the species in green live on all three islands, while the other species live only on one of the islands.

Chapter 4

Scrutinizing the linear variable importance of local explanations of non-linear models with animated linear projections

Now we can be confident that the radial tour leads to better analysis of variable-level attribution to features identified in a projection. We want to increase the interpretability of complex models. Specifically, I suggest a using the radial tour to explore variable sensitivity to the structure identified in linear local explanations of non-linear models.

Artificial Intelligence (AI) has seen a revitalization in recent years from the use of increasingly hard-to-interpret black-box models. In such models, increased predictive power comes at the cost of the opacity of factor analysis and variable interpretability. The loss of interpretability has led to the field of eXplainable AI (XAI). XAI attempts to shed light on these models by providing means for interpreting them. A *local explanation* of a non-linear model gives a point-estimate of linear variable importance in the vicinity of one observation. After creating a model and exacting explanations for each observation, we explore the original variables, the explanation's attribution, and model information side-by-side with interactively display. After identifying an observation of interest, its local

explanation is used as a 1D projection basis. We then manipulate the magnitude of a variable's contribution with a *tour* technique. The tour animates many projections over small changes in the projection basis as it changes the contribution of one variable. Doing so allows an analyst to visually explore the data through the lens of this local explanation and test the variable support where the explanation seems valid. The interactive application and code facilitating this methodology is available are the **R** package **cheem**, available on CRAN.

4.1 Introduction

There are different reasons and emphases to fit a model. Breiman and Shmueli (Breiman, 2001; Shmueli, 2010) introduce the idea of distinguishing modeling based on its purpose; *explanatory* modeling is done for some inferential purpose, while *predictive* modeling focuses more on the predictions of out-of-sample observations. The intended use has important implications for model selection and development. In explanatory modeling, interpretability is vital for drawing inferential conclusions. While predictive modeling may opt for more accurate non-linear models. The use of black-box models is becoming increasingly common, but not without their share of controversy (O'neil, 2016; Kodiyian, 2019). However, the loss of interpretation should not be taken lightly.

Interpretability is vital for exploring and protecting against potential biases in any model. For instance, models regularly pick up on biases in the training data that have observed influence on the response variable, which is then built into the model. Such biases include sex (Dastin, 2018; Duffy, 2019), race (Larson et al., 2016), and age (Díaz et al., 2018). Variable-level interpretability of models is essential in the evaluation models for such biases.

Another concern is that of data drift. Data drift is an unexpected shift in support of the variables. Non-linear models are regularly more sensitive to these changes. The interpretability of the model means more transparency to see where models' predictions may be plausible or completely unreliable.

Explainable Artificial Intelligence (XAI) is a recent branch of research that tries to increase the interpretability of black-box models. One way to do so is to use *local explanations*, which

take a variable attribution approach to bring transparency to a model. Local explanations attempt to approximate linear variable importance at the location of one observation. Even with a linear space or local approximation, the number of terms is usually sizable, thus challenging to visualize comprehensively.

In multivariate data visualization, a *tour* (Asimov, 1985; Buja and Asimov, 1986; Lee et al., 2021) is a sequence of linear projections of data onto a lower-dimensional space. Tours are viewed as an animation over minor changes to the projection basis. Structure in a projection can then be explored visually to see which variables contribute to the formation of that structure. The intuition is similar to watching the shadow of a hidden 3D object change as the object is rotated; watching the shape of the shadow change conveys information of the structure and features of the object.

There are various types of tours distinguished by the generation of projection bases. In a *manual* tour (Cook and Buja, 1997; Spyrisson and Cook, 2020), the path is defined by changing the contribution of a selected variable. Applying tours to models has been done in a couple of contexts. Specifically for exploring various statistical model fits and classification boundaries (Wickham, Cook, and Hofmann, 2015), and using tree- and forest-based approaches as a projection pursuit index to generate a tour basis paths (Lee et al., 2013; Silva, Cook, and Lee, 2021).

The proposed approach uses the radial, manual tour to scrutinize a local explanation. After identifying an observation of interest, its explanation can be evaluated by testing the support of the structure identified by changing variable contribution with the radial tour. We provide a free and open-source R package **cheem** with an interactive application to facilitate analysis. We supply toy and modern datasets case studies for classification and regression tasks.

The change in the projection basis might feel similar to counterfactual, what-if analysis, such as *ceteris paribus* (Biecek, 2020). This phrase, Latin for “other things held constant” or “all else unchanged”, shows how an observation’s prediction would change from a marginal change in one explanatory variable given that other variables are held constant. It ignores correlations of the variables and imagines a case that was not observed. In contrast, our

approach is a geometric explanation of the factual; it varies contributions of the variables by rotating the basis, a reorientation of the data object. Another difference is that the basis must remain orthonormal. That is to say, when the contribution of one variable decreases, the contributions of others necessarily increase such that there is a complete component in that direction.

The remainder of this paper is organized as follows. The following section, [Local explanation statistics](#), covers the background of the local explanation, SHAP, and the traditional visuals produced from it. [Tours and the radial tour](#) digs deeper into these animations of continuous linear projections. The section [Application Design](#) discusses the visual layouts, how they facilitate analysis, data preprocessing, and package infrastructure. The section [Case Studies](#) illustrates several applications of this method. We conclude with a [Discussion](#) of the insights we draw from classification and regression tasks.

4.2 Local explanation statistics

Consider a highly non-linear model. At face value, it is hard to say which variable(s) are sensitive to crossing a classification boundary or identify which variables caused an observation to have a relatively extreme residual. Local explanations shed light on these cases by approximating linear variable importance in the vicinity of one observation.

Figure six of Arrieta et al. (2020) gives comprehensive summarization of the taxonomy and literature of explanation techniques. The figure includes a large number of model-specific explanations such as deepLIFT, (Shrikumar et al., 2016; Shrikumar, Greenside, and Kundaje, 2017) a popular recursive method for estimating importance in neural networks. There are fewer model-agnostic explanations, of which LIME, (Ribeiro, Singh, and Guestrin, 2016) SHAP, (Lundberg and Lee, 2017) and their variants are popular.

These instance-level explanations are used in various ways depending on the data. In images, saliency maps overlay or offset a heatmap indicating necessary pixels (Simonyan, Vedaldi, and Zisserman, 2014). For instance, snow may be highlighted when distinguishing if a picture contains a wolf or husky. In text analysis, word-level contextual sentiment analysis can be used to highlight the sentiment and magnitude of influential words (Vanni

et al., 2018). In the case of numeric regression, they are used to explain variable additive contributions from the model intercept to the observation’s prediction (Ribeiro, Singh, and Guestrin, 2016).

4.2.1 SHAP and tree SHAP

SHapley Additive exPlanations (SHAP) approximates the variable importance in the vicinity of one observation by taking the median importance of a subset of permutations in the explanatory variables. This idea stems from the field of game theory, where Shapley (1953) devised a method to evaluate an individual’s contribution to cooperative games by permuting the players that contribute to the score.

To illustrate SHAP and its original use, explaining the difference between the intercept and an observation’s prediction, we use soccer data from FIFA 2020 season (Leone, 2020). We have 5000 observations of nine skill measures (after aggregating highly correlated variables). A random forest model is fit to regress the log wages, in 2020 Euros, from the skill measures. We then extract the SHAP values of a star offensive player (L. Messi) and defensive player (V. van Dijk). We expect to see a difference in the attribution of the variable importance across the two positions of the players.

Figure 4.1 shows the SHAP values of these players. Panel a) shows these players receive a sizable difference in wages. Panel b) shows the underlying distribution of the SHAP attributions while permuting the explanatory variables, with the medians being the SHAP values. In the light of the player position, the difference in the variable importance makes sense; offense and movement skills are more important for the offensive player, while defensive and power skills are more informative to the model for explaining the prediction of the defensive player. We would likewise expect the profile of variable importance to be unique for star players of other positions, such as goalkeepers or middle fielders. Panel b) shows a simplified break-down plot (Gosiewska and Biecek, 2019), where a local explanation is used to additively explain the difference from the intercept to the observation’s prediction. Such additive approaches will show asymmetry in the variable ordering, so we opt to fix the order to panel a) by decreasing the sum of the SHAP values.

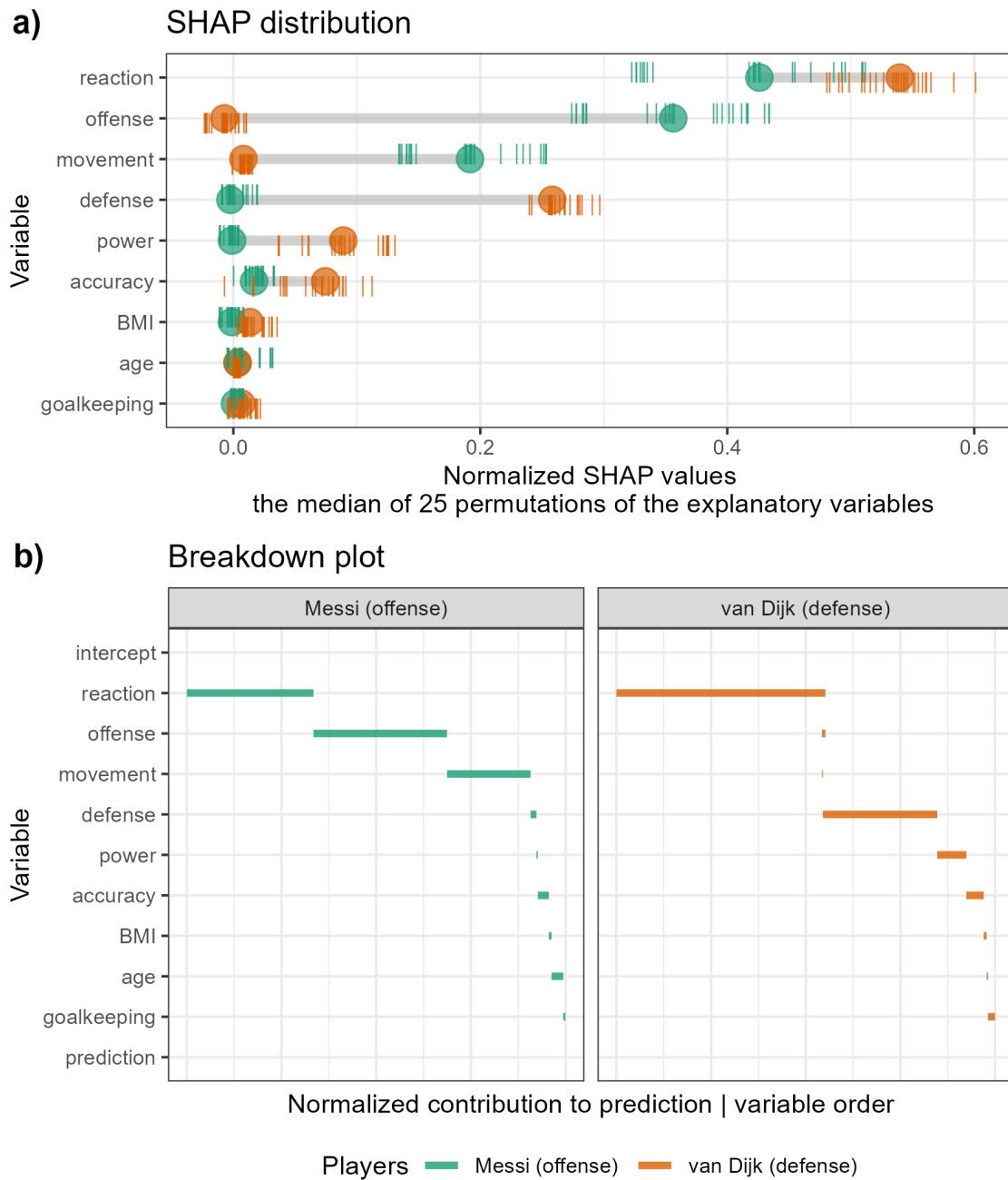


Figure 4.1: Illustration of the distribution of SHAP attributions and a break-down plot. From FIFA 2020 data, a random forest model regresses wages from nine skill attributes for a star offensive and defensive player. The players have very different salaries, but a) shows the distributions of 25 permutations in the explanatory variables. The medians of these distributions are the final SHAP values. The variable importance differs across the exogenous information of player position. These explanations make sense; the variable importances seem realistic given the player's positions. b) Break-down plots of the observations using their explanations to additively cover the difference between the model intercept and the observation predictions.

In summary, this figure highlights how local explanations bring interpretability to a model, at least in the vicinity of their observations. In this instance, two players with different positions receive different profiles of variable importance to explain the prediction of their wages. In application, we apply *tree SHAP*, a variant of SHAP enjoys a lower computational complexity (Lundberg, Erion, and Lee, 2018). Tree SHAP is only compatible with tree-based models; we illustrate random forests. The following section will use normalized explanations as the starting projection basis to further scrutinize the explanation.

4.3 Tours and the radial tour

A data visualization *tour* animates many linear projections over small changes in the basis. One of the critical features of the tour is the object permanence of the data points; one can track the relative changes of observations as the basis moves, as opposed to discretely jumping to an orthogonal view with no intermediate information. There are various types of tours that are distinguished by selecting their basis paths (Lee et al., 2021; Cook et al., 2008).

4.3.1 Manual tours and its radial case

The manual tour (Cook and Buja, 1997) defines its basis path by manipulating a selected variable's contribution to the basis. A manipulation dimension is appended onto the projection plane, giving a full contribution to the chosen variable. The bases are then selected based on rotating this newly created manipulation space. A crucial feature of the manual tour is that it allows users to control the variable contributions of the basis. Such manipulations can be selected and queued in advance or selected on the spot for human-in-the-loop analysis (Karwowski, 2006). However, this navigation is relatively time-consuming due to the vast volume of the display space. It is advisable to use this method to explore the sensitivity of the variable contribution to a previously identified feature of interest. In this case, the projection of the normalized explanations is the feature of interest.

More generally, the manual tour can change the contribution of a variable to the display dimensions. We will apply a more directed interaction, namely, a *radial* tour. In a radial

tour, the selected variable is allowed to change its magnitude of contribution but not its angle; it must move along the direction of its original contribution.

4.4 Cheem viewer

Below we illustrate the two primary displays of the cheem viewer application: the global view and the tour view. Then we cover what we take away from the classification and regression tasks. Lastly, we discuss the preprocessing of the data before application runtime.

4.4.1 Global view

The global view provides an essential context of all observations and facilitates the exploration of the separability of the data- and attribution-spaces. While the comparison of these spaces is interesting, the global view's purpose is to enable the selection of observations. The local explanation of these points will be explored in more detail.

An approximation of these spaces is given as the first two principal components of their respective spaces. Model information, the observed response by its prediction, is also provided. The orientation and magnitude of the variables are inscribed on a unit circle. Misclassified observations are circled in red if applicable. Linked brushing between the plots and tabular display of select points facilitates exploration of the spaces and the model. A single 2D projection will not encompass all of the structure of higher-dimensional space. However, it is a reasonable summarization given the real task at hand; the selection of observations to explore further.

4.4.2 Radial cheem tour

The global view facilitated the selection of a primary and optional comparison observation. The variable-level attribution of the primary observation is normalized and used as the initial 1D basis in a radial tour. This is an approximation of the contributions of the linear variables that best explain the difference between the model intercept and an observation's prediction, not the local shape of the model surface.

The initial frame is the normalized SHAP values of the primary observation. The current projection basis is depicted as the width of a bar, the variable's contribution to the horizontal axis. The normalized values of all observations are shown as vertical parallel coordinate plots.

The radial tour creates a basis path by varying the contribution of a selected variable, fully into and out of a projection frame. Doing so tests an individual variable's sensitivity to the structure identified by the local explanation. The default variable selected has the largest discrepancy between the attribution of primary and comparison observations. The following sections elaborate on the takeaways from applying this approach in classification and regression tasks. Now that we have introduced the global view and corresponding cheem radial tour, let us discuss the differences between the classification and regression cases.

4.4.3 Classification task

What information do we glean from using this method on a classification task? Typically we select a misclassified observation compared to a correctly classified point nearby in data space. The initial frame is the linear attribution of that observation's local explanation. By default, the manual tour varies the contribution of the variable with the largest difference between the primary and comparison observation; we can test the sensitivity of each variable to structure identified by the local explanation; we are exploring the support of the explanation, evaluating the support or robustness of the prediction.

4.4.4 Regression task

In the regression case, the global view can be colored on a statistic to highlight the explanation space's structure. For this purpose, we include residuals, log Mahalanobis distance of data space (a measure of outlyingness), and the correlation of the attribution projection with the observed response. In the radial tour, the horizontal positions are the same, the basis projection of the radial tour. The vertical position is fixed to the observed response variable and residuals in the middle and right panels. Correspondingly, the



Figure 4.2: Display illustrating the classification case. Plots are colored on predicted class, and red circles indicate misclassified observations. The radial tour is a 1D projection starting at the normalized tree SHAP values of the primary point. The first frame is the linear-variable importances that best describe the difference from model intercept to this observation's prediction. We probe the support of the variable contributions by selecting a variable to vary the contribution.

CHAPTER 4. SCRUTINIZING THE LINEAR VARIABLE IMPORTANCE OF LOCAL EXPLANATIONS OF NON-LINEAR MODELS WITH ANIMATED LINEAR PROJECTIONS

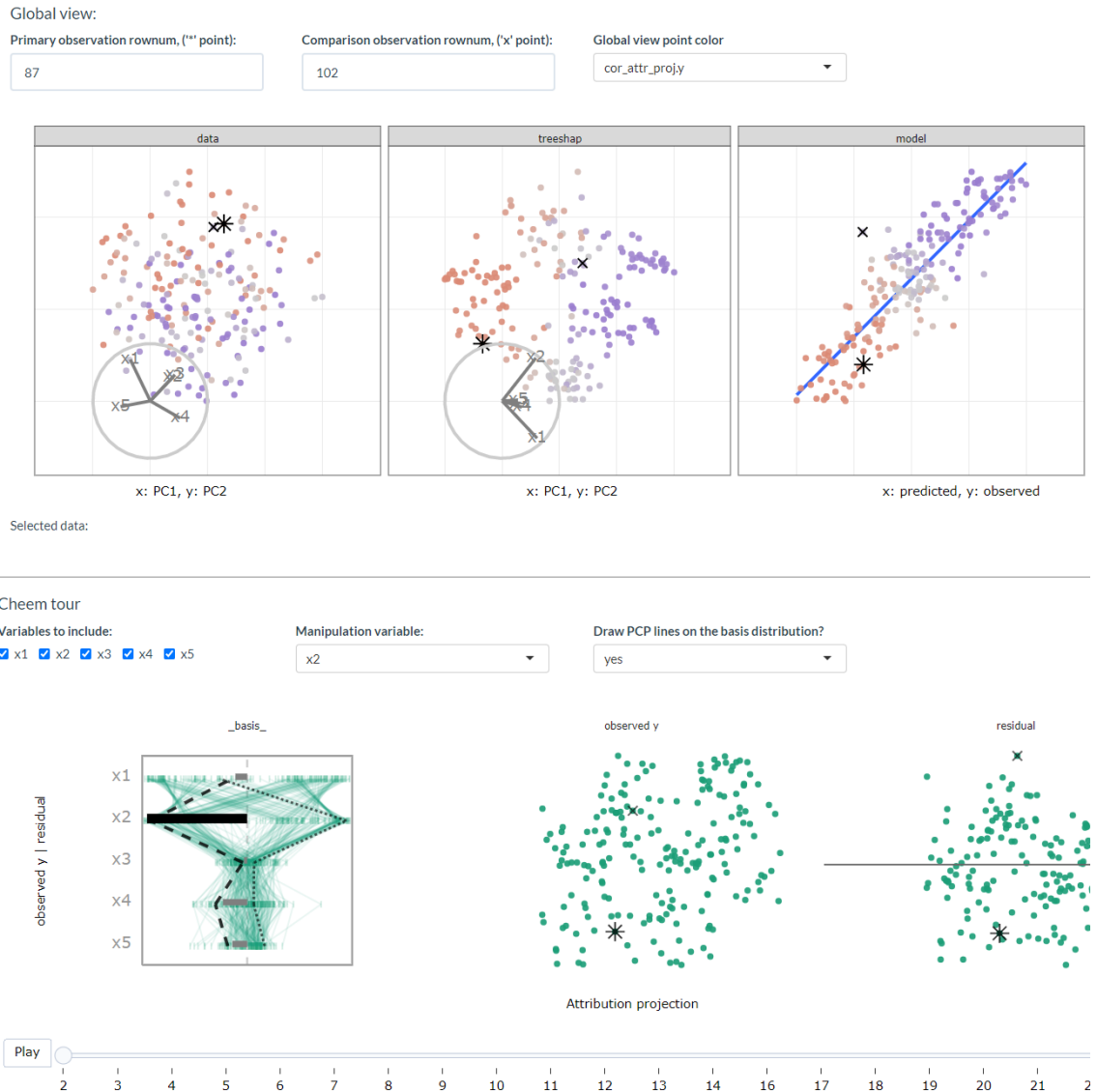


Figure 4.3: Display of the regression task. The global view can be colored on the correlation of the attribution projection and observed response. In the tour, the horizontal values are the same as the classification case; the projection through the basis. The vertical position is now mapped to the observed y and residuals.

display changes from univariate density to 2D scatterplot. The basis is still one component (horizontal) independent of the vertical position.

4.4.5 Interactive features

The application has several reactive inputs that affect the data used, aesthetic display, and tour manipulation. These reactive inputs make the software flexible and extensible. The

CHAPTER 4. SCRUTINIZING THE LINEAR VARIABLE IMPORTANCE OF LOCAL EXPLANATIONS OF NON-LINEAR MODELS WITH ANIMATED LINEAR PROJECTIONS

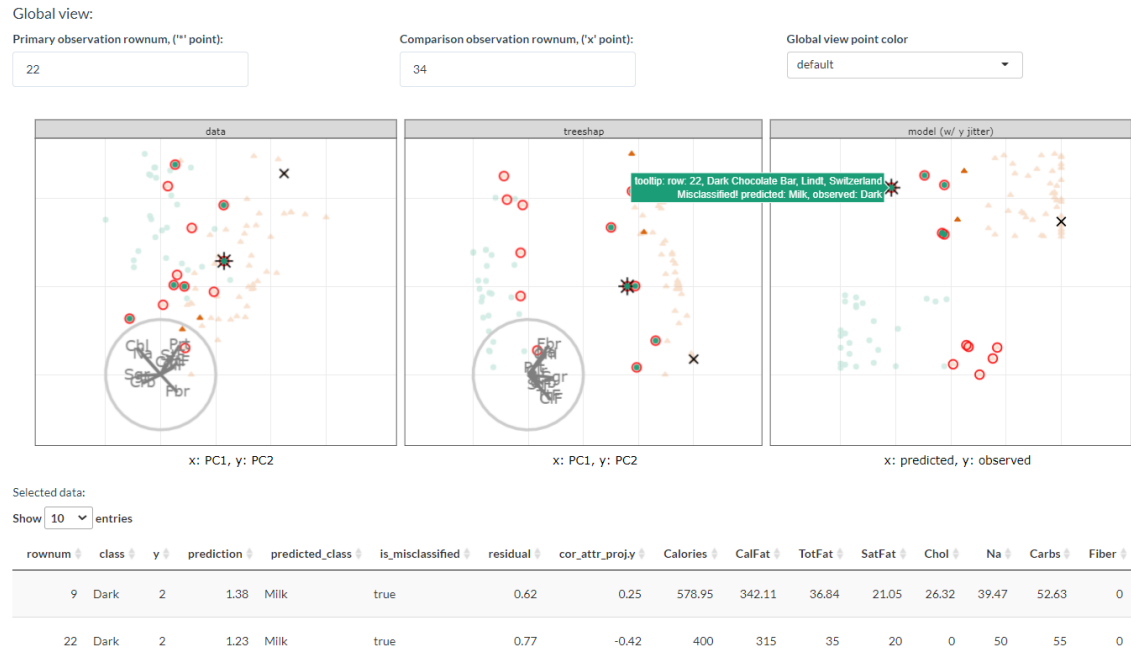


Figure 4.4: Illustration of data explorations interactions in the global view. This view has linked brushing, where observations selected in one facet are highlighted in the other facets and populate an interactive tabular display below. Tooltips display when hovering over an observation.

application also has more exploratory interactions to help link points across displays and reveal structure found in different spaces.

A tooltip displays observation number/name and classification information while the cursor hovers over a point. Linked brushing allows the selection of points (left click and drag) where those points will be highlighted across plots. The information corresponding to the selected points is populated on a dynamic table. These interactions aid exploration of the spaces and, finally, identification of a primary and comparison observation.

4.4.6 Preprocessing

It is vital to mitigate the render time of visuals, especially when users may want to iterate many times. All computational operations should be prepared before runtime. The work remaining when an application is ran is solely reacting to inputs and rendering of visuals and tables. Below we discuss the steps and details of the reprocessing.

- **Data:** a complete numerical matrix; explanatory and response variable. An optional categorical variable can be mapped to the color and shape of observations. Explanatory variables are scaled in visualization after modeling or creating local explanations.
- **Model:** any model can be used with this method. Currently, we apply random forest models via the package **randomForest** [Liaw and Wiener (2002)] for compatibility with the local explanation, which requires tree-based models.
- **Local explanation:** any model-compatible linear explanation could be used. We apply tree SHAP, a more computationally efficient variant of SHAP, compatible with tree-based models. Tree SHAP was calculated with the package **treeshap** [Kominsarczyk et al. (2021), hosted on GitHub only]. The global view shows all observations in attribution space, requiring the variable importance from *all* observations rather than just one.

The time to preprocess the data will vary significantly with the model and local explanation. For reference, the FIFA data, 5000 observations of nine explanatory variables, took 2.9 seconds to fit a random forest model of modest hyperparameters. Extracting the tree SHAP values of each observation took 254 seconds combined. PCA and statistics of the variables and attributions took 0.6 seconds. These runtimes were from a non-parallelized R session on a modern laptop, but suffice to say that the bulk of the time will be spent on the local attribution. An increase in model complexity or data dimensionality will quickly become an obstacle. With its reduced computational complexity, this makes tree SHAP a good candidate to start with. Alternatively, the package **fastshap** (Greenwell, 2020) claims extremely low runtimes, which are attributed to fewer calls to the prediction function, partial implementation in C++, and efficient use of logical subsetting.

4.4.7 Package infrastructure

The above-described method and application are implemented as an open-source **R** package, **cheem** available on [CRAN](#). Preprocessing was facilitated with models created via **randomForest** (Liaw and Wiener, 2002), and explanations calculated with **treeshap** (Kominsarczyk et al., 2021). The application was made with **shiny** (Chang et al., 2021). The tour visual

is built with **spinifex** (Spyrison and Cook, 2020). Both views are created first with first with **ggplot2** (Wickham, 2016) and then rendered as interactive HTML widgets with **plotly** (Sievert, 2020). **DALEX** (Biecek, 2018) and the free ebook, *Explanatory Model Analysis* (Biecek and Burzykowski, 2021) were a huge boon to understanding local explanations and how to apply them.

4.4.8 Installation and getting started

The following R code will help getting up and running:

```
## Download the package
install.packages("cheem", dependencies = TRUE)

## Restart the R session so the IDE has the correct directory structure
restartSession()

## Load cheem into session
library("cheem")

## Try the app
run_app()

# Processing your data

## Install treeshap from github, to use as a local explainer
remotes::install_github('ModelOriented/treeshap') ## Local

## Follow the examples in cheem_ls()
?cheem_ls
```

4.5 Case studies

To illustrate the use of the cheem method, we apply it to modern datasets, two classification examples and then two of regression.

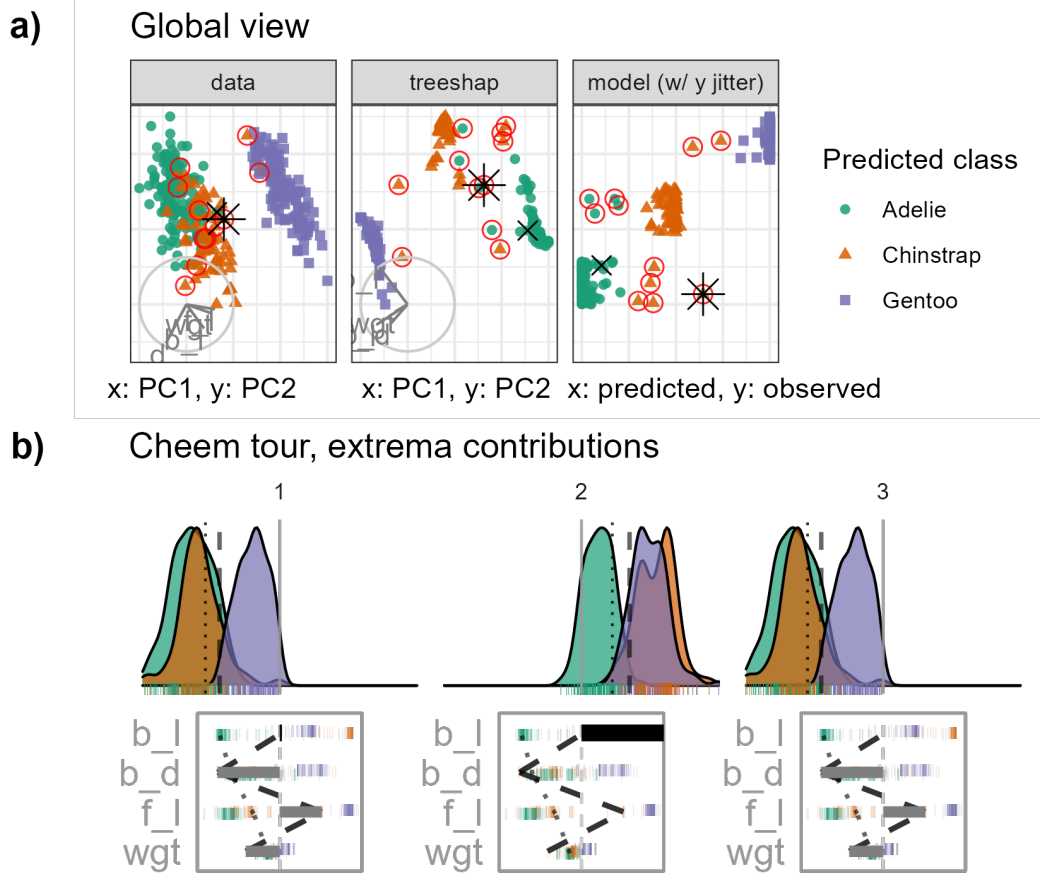


Figure 4.5: Species classification of Palmer penguin data. We select a chinstrap penguin that is mislabeled as an adelie. By varying the contribution to bill length, we observe the explanation does not hold when bill length has a significant contribution. The .mp4 animation of this tour can be found at github.com/nspyrison/cheem_paper/blob/main/figures/case_penguins.mp4

4.5.1 1) Penguin, species classification

Palmer penguins data (Gorman, Williams, and Fraser, 2014; Horst, Hill, and Gorman, 2020) consist of 330 observations across four physical measurements of three species of penguins foraging near Palmer Station, Antarctica. A random forest model was fit, classifying the species of the penguin given the physical measurements.

In figure 4.5, a misclassified point is contrasted with a correctly classified point of its observed class nearby in data-space. The attribution space from the tree SHAP local explanations is a more separable space, where the comparison is squarely in the middle of the orange distribution. The primary observation is between the predicted and observed

clusters, a sign of uncertainty in the prediction. The tour varies the contribution of bill length (`b_l`) as this variable differs most from the contribution of the comparison observation. Downplaying the contribution of bill length is crucial to the linear explanation of this observation being misclassified.

4.5.2 2) Chocolates, milk/dark chocolate classification

The chocolates dataset consists of 88 observations of 10 nutritional measurements from their labels. Each of which was labeled as being either milk or dark chocolates. We can see if a manufacturer accurately portrays the chocolate with this data. We are curious to see if chocolates that nutritionally look like milk chocolates are labeled as dark chocolates, which may hold a higher market value. We should note that not all chocolates consist wholly of chocolate. The addition of other ingredients will decrease the predictive power of the model nutritional explanatory variable. A random forest model is fit classifying the type of chocolate. We selected a chocolate labeled dark, through predicted to be milk chocolate compared with a chocolate labeled 85% cocoa.

Figure 4.6 similarly shows that attribution-space is more separable than data-space. Interestingly, the class imbalance that we suspected was not observed; there are only six chocolates labeled as dark and predicted as milk, while eight of the inverse case. Calories from fat is the variable with the largest difference in treeshap attribution between these points. In this case, it feels strange to call the selected observation a misclassification of the model. There are plausible reasons that a manufacturer has incentives to cut corners and label their products different than what they are. This feels more like a measurement theory-related problem. In this case, the candy is being sold as dark chocolate, while nutritional value more closely resembles milk chocolates.

4.5.3 3) FIFA, wage regression

The 2020 season FIFA data (Leone, 2020; Biecek, 2018) contains many skill measurements of soccer/football players and wage information. After aggregation of the skill measurements, we regress the log wages [2020 euros] given just the skill aggregates. The model was fit from 5000 observations of the nine skill aggregates before being thinned to 500 players to

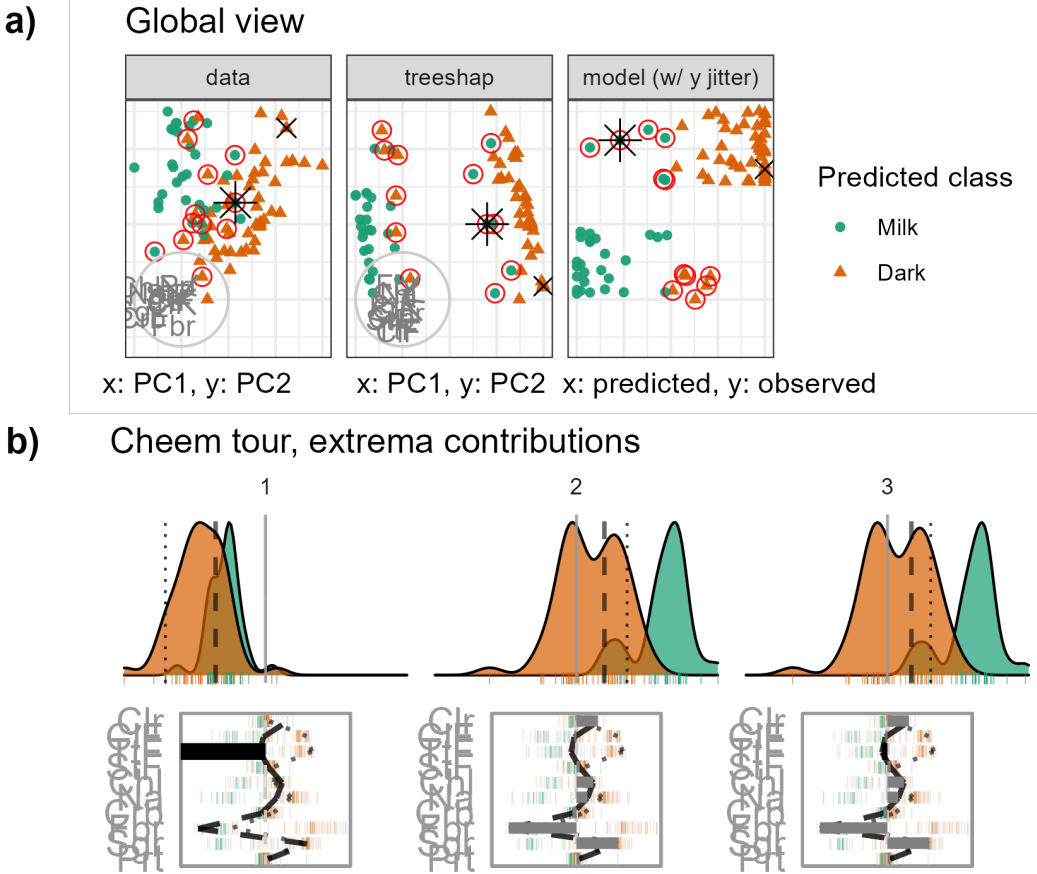


Figure 4.6: Chocolates data type classification (milk or dark). We select a chocolate labeled as dark though a random forest model predicts it to be milk chocolate in light of the values on the nutritional label. We vary the contribution of calories from fat. Animated tour can be found at github.com/nspyrison/cheem_paper/blob/main/figures/case_chocolates.mp4.

mitigate occlusion and render time. We compare a leading offensive fielder (L. Messi) with that of a top defensive fielder (V. van Dijk), the same observations were used in figure ??.

With figure 4.7, we will test the premise of the local explanation. If we remove reaction and movement skills from the basis, offense skills are almost singularly important for explaining the offensive player. We vary the contribution of offensive skills. Offensive skills are removed in the tour (panel b, frame 3), and Messi is no longer separated from the group. We also notice that accuracy has rotated into the frame, maintaining some separability.

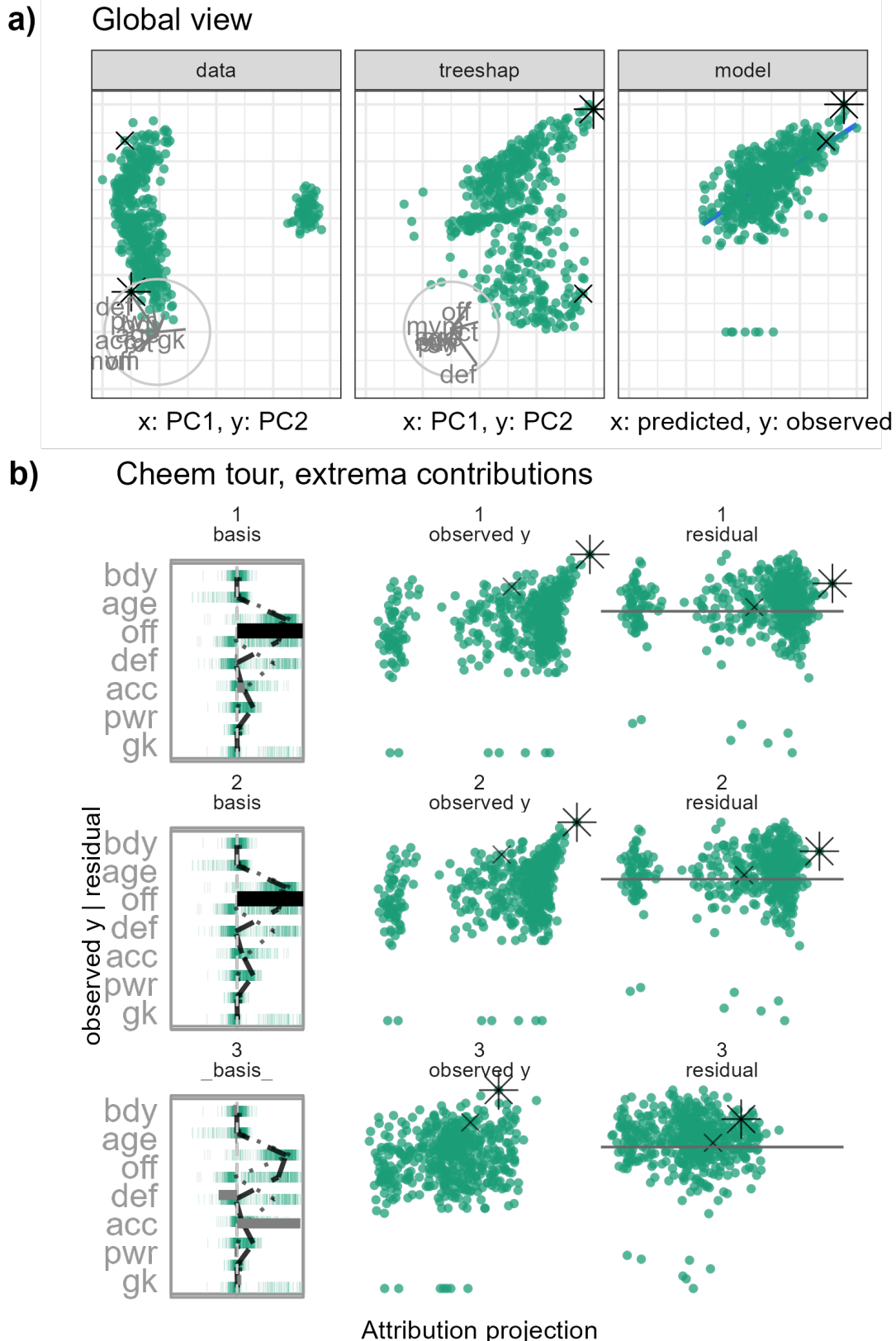


Figure 4.7: FIFA 2020, regressing log wages [2020 Euros] from aggregations of skill measurements. The primary observation is a star offensive player (L. Messi) compared with a top defensive player (V. van Dijk). The animate radial tour can be found at github.com/nspyrison/cheem_paper/blob/main/figures/case_fifa.mp4

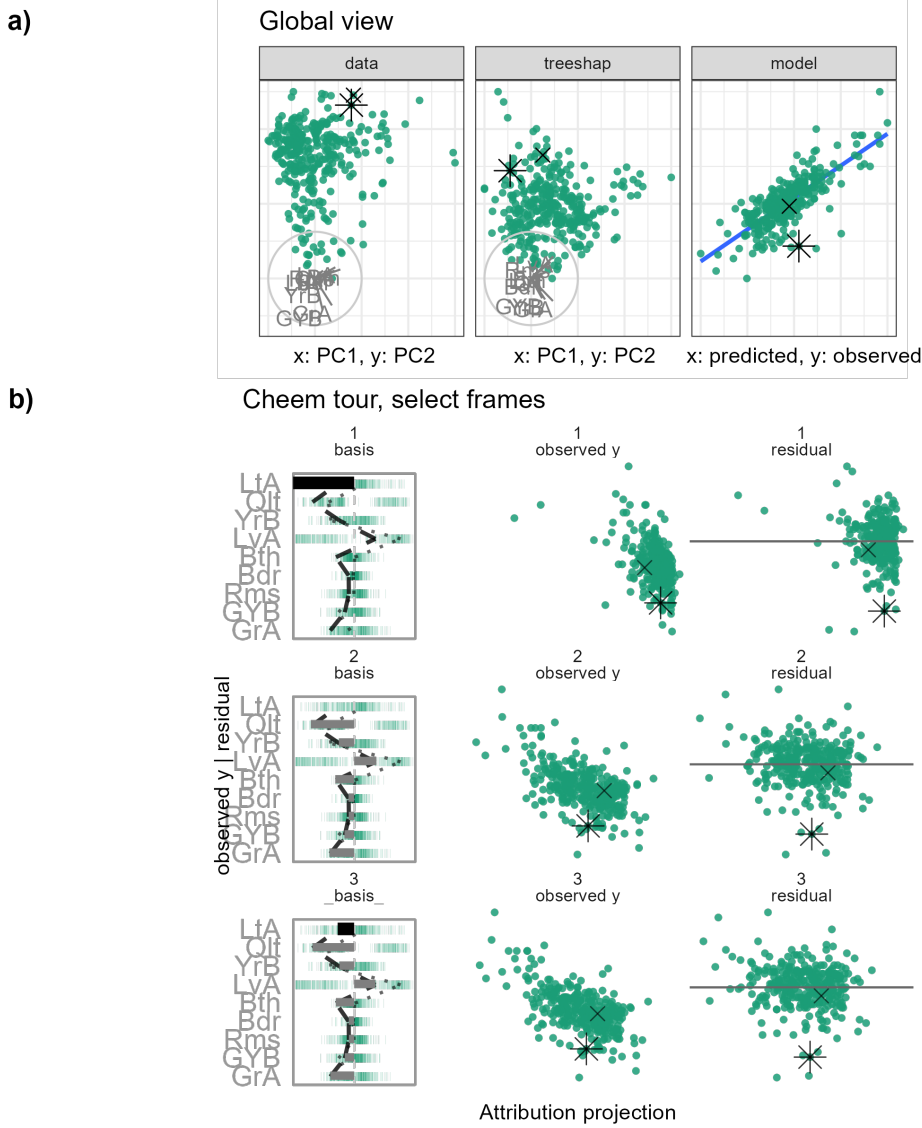


Figure 4.8: Ames housing 2018 regressing log sales price [2018 USD]. Because the SHAP values are relatively well distributed across the variables, there is a lot of redundant information to explain the gap between select observations. This case may not be ideal for the cheem methodology, though we did find a near singular frame in the manual tour not, something we came looking for, but certainly, an exciting feature to find. The corresponding animation is at github.com/nspyrison/cheem_paper/blob/main/figures/case_ames2018.mp4

4.5.4 4) Ames housing 2018, sales price regression

Ames 2018, housing data was subset to North Ames (the neighborhood with the most house sales). The remaining are 338 house sales across nine variables. Using interaction from the global view, we select a house with an extreme negative residual and an accurate observation close to it in the data.

Figure 4.8 shows the global view and extrema of the tour. The horizontal distance in the tour did not show a significant disparity between our selected points. This is not particularly surprising as most variables have a sizable contribution. Rotating any one variable out of the frame will rotate other vital variables into the frame, preserving most of the distance from intercept to prediction. However, the tour has revealed an interesting feature worth discussing. Notice that the observations pivot about the origin, the basis roughly halfway between bases in frames one and two of panel b) the data is near a singular profile. This means that there is a basis orthogonal to this point that describes sizable variation. Knowing these singular bases can point toward others with meaningful data variation.

4.6 Discussion

The need to maintain the interpretability of black-box models is evident. One aspect uses local explanations of the model in the vicinity of an observation. Local explanations approximate the linear variable importance to the model. Our contribution is to assess explanations by examining the support by varying the contributions with a radial tour. First, a global view visualizes approximations of the data space, explanation space, model predictions side-by-side, using dynamic interaction to compare and contrast and identify primary and comparison observations of interest. The normalized linear importance from the explanation of the primary observation becomes the feature of interest to further explore with the radial tour. The tours explore the variable sensitivity to the structure identified in the explanation.

We have illustrated this method on random forest models using the tree SHAP local explanation, while it could be generally used with any compatible model-explanation pairing. We apply it to the classification and regression tasks. We have created an open-source **R** package **cheem**, available on [CRAN](#), to facilitate preprocessing and exploration with the described interactive application. Toy and real data are provided, or upload your data after preprocessing.

4.7 Acknowledgments

We would like to thank Professor Przemyslaw Biecek for his input early in the project and to the broader MI² lab group for the **DALEX** ecosystem of **R** and **Python** packages. This research was supported by Australian Government Research Training Program (RTP) scholarships. Thanks to Jieyang Chong for helping proofread the article.

The namesake, Cheem, refers to a fictional race of humanoid trees from Doctor Who lore. **DALEX** pulls on from that universe, and we initially apply tree SHAP explanations specific to tree-based models.

4.8 References

Chapter 5

Conclusion

We know that visualizing data is more robust than numerical summarization alone. It provides a means to rapidly get a feel for the data, check for erroneous values, and confirm model assumptions. But visualizing data spaces becomes increasingly complex as dimensionality increases. Linear dimension reduction and especially dynamic animations of linear projections, tours, seems to be a fruitful way to extend data visualization as dimensionality increases. Previously we haven't had a means of testing the sensitivity of individual variables' contribution to the structure in one embedding. In Chapter 2 introduced the **spinifex** package, which facilitates user-controlled manual tours and extends the exporting of any tour, interoperability with **tourr**. Use of the radial, manual tour does sizably improve the accuracy on variable-level supervised cluster separation task compared with PCA and the grand tour. Chapter @ref(ch-efficacy_radial_tour) covers the with-in participants user study that led to this conclusion. Finally, we extended the use of the manual tour to increase the interpretability of non-linear models by using it to explore their local explanations in the package **cheem** is discussed in 4.

5.1 Software development

The **spinifex** package facilitates the preprocess transformations with **scale_*** functions, identifies features with **basis_*** functions, and allows user-control over variable contributions to the basis with manual tours. It creates a framework for layered creation of tour

visuals with `proto_*` functions will feel at home to **ggplot2** users. Manual tours and those created from **tourr** can be rendered and exported as interactive HTML widgets, .gif, or .mp4 files. Vignettes and interactive an application help users get started. It has been downloaded over 14,400 times from CRAN between 09 April 2019 and 28 November 2021. The package is available on [CRAN](#) with vignettes and version notes on its [pkgdown](#) site. My contributions **spinifex** and **tourr** won the ACEMS Impact and Engagement Award, 2018.

In the **cheem** package, I suggest using manual tours to extend the interpretability of black-box models by exploring their local explanations. A workflow is developed to facilitate the creation of a random forest model, calculating tree SHAP local explanations for each observation. An interactive application illustrates the purposed visual and analysis from several datasets or upload your data after processing. Local explanations are evaluated through testing the sensitivity of the variables to the structure identified in the explanation. **cheem** was recently uploaded to [CRAN](#) and has a corresponding [pkgdown](#) site.

5.2 Further extensions

In addition to controlling the contribution of a single variable, it may be insightful to able to change contributions of several at once (manipulating on a linear combination). A sort of dimension reduction tour that would append several manual tours together, zeroing the contributions of variables one at a time may prove interesting in the vicinity of the a features intrinsic dimensionality.

There are direct natural extensions to **spinifex**, such as extending the type of protos available, such as adding a text table of the basis, convex hulls, alpha hulls, and a ‘high density region’ display where the bulk of the data is shown as density contour, while the outer most observations are displayed as points (Hyndman, 1996). An additional interpolation of the manual tour could correlate the frame number with the magnitude of a radial tour; the first frame would contain zero magnitude, and the last contains a full contribution, while the default starting frame would initial value.

Experiencing tours as 3D scatterplots in extended reality with stereoscopically true head tracking may be fruitful. (Nelson, Cook, and Cruz-Neira, 1998) explore 2D tour in virtual reality. Other works view 3D scatterplot tours on 2D displays (Yang, 1999, 2000). It would be interesting to see modern implementations using WebGL, Mozilla A-frame, or Unity. One concern would be trying to keep hardware and software as generalized as possible.

Similarly, **cheem** analysis could be generalized to a broader range models and local explanations. The models and local explanations facilitated by **DALEX::explain()** seems to be a good starting point (Biecek, 2018; Biecek and Burzykowski, 2021). Alternatively, there may be other statistics that better show the structure identified by explanations that could be added.

5.3 Other contributions

In addition to the research discussed around the thesis of the manual and radial, manual tour other notable contributions during my candidature include:

- *The state-of-the-art on tours for dynamic visualization of high-dimensional data* (Lee et al., 2021), WIREs Computational Statistics. Review of current tour methods. I contributed writing and manual tour frame discussing manual tours.
- *“Is IEEE VIS that good?” On key factors in the initial assessment of manuscript and venue quality* (Spyrison, Lee, and Besançon, 2021). A survey IEEE VIS authors, how they source articles, decide which to read, and evaluate venue quality. We find low evidence that sentiment changes across academic positions for these topics and provide commentary and discussion on the effects of “publish or perish” environment, standard author and journal metrics, and the need to publish “null” findings and replication studies.
- *Intraday effect of COVID-19 restrictions on Melbourne electricity consumption* (Barrow, Chong, and Spyrison, 2020). We corroborate that the Victorian interday effect on energy consumption did not change, and novelly find that the intraday distribution of energy consumption does change. Namely, we find a statistically significant change

in the height of the morning and evening peak, energy consumption that we posit is due to less strict schedules associated with working from home, absence of commute time, and other employment changes. We were awarded 1st place of hundreds of entries in the insights category of the Melbourne 2020 Datathon.

- Student volunteering at three conferences: UseR!2021 - Online, CHI Down Under 2020 - Online, and UseR!2018 - Brisbane, Australia.

Bibliography

- Adadi, A and M Berrada (2018). Peeking inside the black-box: a survey on explainable artificial intelligence (XAI). *IEEE access* **6**. Publisher: IEEE, 52138–52160.
- Allaire, JJ, Y Xie, J McPherson, J Luraschi, K Ushey, A Atkins, H Wickham, J Cheng, W Chang, and R Iannone (2020). *rmarkdown: Dynamic Documents for R*. <https://github.com/rstudio/rmarkdown>.
- Anscombe, FJ (1973). Graphs in Statistical Analysis. *The American Statistician* **27**(1), 17–21. (Visited on 12/19/2018).
- Arrieta, AB, N Díaz-Rodríguez, J Del Ser, A Bennetot, S Tabik, A Barbado, S García, S Gil-López, D Molina, and R Benjamins (2020). Explainable Artificial Intelligence (XAI): Concepts, taxonomies, opportunities and challenges toward responsible AI. *Information Fusion* **58**. Publisher: Elsevier, 82–115.
- Asimov, D (1985). The Grand Tour: a Tool for Viewing Multidimensional Data. *SIAM journal on scientific and statistical computing* **6**(1), 128–143.
- Barrow, M, J Chong, and N Spyris (2020). Changes to Victorian Intraday Electricity Demand Following COVID-19 Restrictions. In: *Melbourne Datathon 2020, Insights category*, pp.4. <https://www.overleaf.com/project/5f614799515ac0000119daf7> (visited on 08/21/2021).
- Bertini, E, A Tatu, and D Keim (2011). Quality metrics in high-dimensional data visualization: An overview and systematization. *IEEE Transactions on Visualization and Computer Graphics* **17**(12). Publisher: IEEE, 2203–2212.
- Biecek, P (2018). DALEX: explainers for complex predictive models in R. *The Journal of Machine Learning Research* **19**(1). Publisher: JMLR.org, 3245–3249.

BIBLIOGRAPHY

- Biecek, P (2020). *ceterisParibus: Ceteris Paribus Profiles*. <https://CRAN.R-project.org/package=ceterisParibus>.
- Biecek, P and T Burzykowski (2021). *Explanatory Model Analysis: Explore, Explain, and Examine Predictive Models*. en. Google-Books-ID: rq4SEAAAQBAJ. CRC Press.
- Breiman, L (2001). Statistical modeling: The two cultures (with comments and a rejoinder by the author). *Statistical science* **16**(3). Publisher: Institute of Mathematical Statistics, 199–231.
- Buja, A and D Asimov (1986). Grand Tour Methods: An Outline. In: *Proceedings of the Seventeenth Symposium on the Interface of Computer Sciences and Statistics on Computer Science and Statistics*. New York, NY, USA: Elsevier North-Holland, Inc., pp.63–67. <http://dl.acm.org/citation.cfm?id=26036.26046> (visited on 01/09/2019).
- Buja, A, D Cook, D Asimov, and C Hurley (2005). “Computational Methods for High-Dimensional Rotations in Data Visualization”. en. In: *Handbook of Statistics*. Vol. 24. Elsevier, pp.391–413. <http://linkinghub.elsevier.com/retrieve/pii/S0169716104240147> (visited on 04/15/2018-04-15).
- Cattell, RB (1966). The scree test for the number of factors. *Multivariate behavioral research* **1**(2). Publisher: Taylor & Francis, 245–276.
- Chambers, J, W Cleveland, B Kleiner, and P Tukey (1983). Graphical Methods for Data Analysis. eng.
- Chang, W, J Cheng, JJ Allaire, Y Xie, and J McPherson (2020). *shiny: Web Application Framework for R*. <https://CRAN.R-project.org/package=shiny>.
- Chang, W, J Cheng, J Allaire, C Sievert, B Schloerke, Y Xie, J Allen, J McPherson, A Dipert, and B Borges (2021). *shiny: Web Application Framework for R*. R package version 1.7.0. <https://CRAN.R-project.org/package=shiny>.
- Chernoff, H (1973). The Use of Faces to Represent Points in K-Dimensional Space Graphically. *Journal of the American Statistical Association* **68**(342), 361–368. (Visited on 01/05/2019).
- Cook, D and A Buja (1997). Manual Controls for High-Dimensional Data Projections. *Journal of Computational and Graphical Statistics* **6**(4), 464–480. (Visited on 04/15/2018-04-15).

BIBLIOGRAPHY

- Cook, D, A Buja, J Cabrera, and C Hurley (1995). Grand Tour and Projection Pursuit. *Journal of Computational and Graphical Statistics* **4**(3), 155. (Visited on 05/27/2018-05-27).
- Cook, D, A Buja, EK Lee, and H Wickham (2008). “Grand Tours, Projection Pursuit Guided Tours, and Manual Controls”. en. In: *Handbook of Data Visualization*. Berlin, Heidelberg: Springer Berlin Heidelberg, pp.295–314. http://link.springer.com/10.1007/978-3-540-33037-0_13 (visited on 08/21/2018).
- Cook, D, U Laa, and G Valencia (2018). Dynamical projections for the visualization of PDFSense data. *Eur. Phys. J. C* **78**(9), 742.
- Dastin, J (2018). Amazon scraps secret AI recruiting tool that showed bias against women. en. *Reuters*. (Visited on 10/25/2021).
- Díaz, M, I Johnson, A Lazar, AM Piper, and D Gergle (2018). Addressing age-related bias in sentiment analysis. In: *Proceedings of the 2018 chi conference on human factors in computing systems*, pp.1–14.
- Duffy, C (2019). Apple co-founder Steve Wozniak says Apple Card discriminated against his wife. *CNN*. (Visited on 10/26/2021).
- Gabriel, KR (1971). The biplot graphic display of matrices with application to principal component analysis. *Biometrika* **58**(3), 453–467.
- Gorman, KB, TD Williams, and WR Fraser (2014). Ecological sexual dimorphism and environmental variability within a community of Antarctic penguins (genus Pygoscelis). *PloS one* **9**(3). Publisher: Public Library of Science San Francisco, USA, e90081.
- Gosiewska, A and P Biecek (2019). IBreakDown: Uncertainty of model explanations for non-additive predictive models. *arXiv preprint arXiv:1903.11420*.
- Gracia, A, S González, V Robles, E Menasalvas, and T von Landesberger (2016). New Insights into the Suitability of the Third Dimension for Visualizing Multivariate/Multidimensional Data: A Study Based on Loss of Quality Quantification. en. *Information Visualization* **15**(1), 3–30. (Visited on 08/20/2018).
- Greenwell, B (2020). *fastshap: Fast Approximate Shapley Values*. <https://CRAN.R-project.org/package=fastshap>.
- Grinstein, G, M Trutschl, and U Cvek (2002). High-Dimensional Visualizations. en, 14.

BIBLIOGRAPHY

- Horst, AM, AP Hill, and KB Gorman (2020). *palmerpenguins: Palmer Archipelago (Antarctica) penguin data*. <https://allisonhorst.github.io/palmerpenguins/>.
- Hurley, C and A Buja (1990). Analyzing High-Dimensional Data with Motion Graphics. *SIAM Journal on Scientific and Statistical Computing* **11**(6), 1193–1211. (Visited on 11/27/2018).
- Hyndman, RJ (1996). Computing and graphing highest density regions. *The American Statistician* **50**(2), 120–126.
- Karwowski, W (2006). *International Encyclopedia of Ergonomics and Human Factors*, -3 Volume Set. CRC Press.
- Keim, DA (2000). Designing pixel-oriented visualization techniques: Theory and applications. *IEEE Transactions on visualization and computer graphics* **6**(1), 59–78.
- Kirkpatrick, S, CD Gelatt, and MP Vecchi (1983). Optimization by simulated annealing. *science* **220**(4598), 671–680.
- Kodiyan, AA (2019). An overview of ethical issues in using AI systems in hiring with a case study of Amazon’s AI based hiring tool. *Researchgate Preprint*.
- Kominsarczyk, K, P Kozminski, S Maksymiuk, and P Biecek (2021). *treeshap*. original-date: 2020-07-30T19:38:33Z. <https://github.com/ModelOriented/treeshap> (visited on 10/29/2021).
- Larson, J, S Mattu, L Kirchner, and J Angwin (2016). How We Analyzed the COMPAS Recidivism Algorithm. en. *ProPublica*. (Visited on 10/25/2021).
- Lee, S, D Cook, N da Silva, U Laa, N Spryison, E Wang, and HS Zhang (2021). The state-of-the-art on tours for dynamic visualization of high-dimensional data. en. *WIREs Computational Statistics* **n/a**(n/a). _eprint: <https://onlinelibrary.wiley.com/doi/pdf/10.1002/wics.1573>, e1573. (Visited on 12/10/2021).
- Lee, YD, D Cook, Jw Park, and EK Lee (2013). PPtree: Projection pursuit classification tree. *Electronic Journal of Statistics* **7**. Publisher: Institute of Mathematical Statistics and Bernoulli Society, 1369–1386.
- Leone, S (2020). *FIFA 20 complete player dataset*. en. <https://kaggle.com/stefanoleone992/fifa-20-complete-player-dataset> (visited on 08/23/2021).

BIBLIOGRAPHY

- Liaw, A and M Wiener (2002). Classification and regression by randomForest. *R news* **2**(3), 18–22.
- Liu, S, D Maljovec, B Wang, PT Bremer, and V Pascucci (2017). Visualizing High-Dimensional Data: Advances in the Past Decade. *IEEE Transactions on Visualization and Computer Graphics* **23**(3). Conference Name: IEEE Transactions on Visualization and Computer Graphics, 1249–1268.
- Lubischew, AA (1962). On the use of discriminant functions in taxonomy. *Biometrics*, 455–477.
- Lundberg, S and SI Lee (2017). A unified approach to interpreting model predictions. *arXiv preprint arXiv:1705.07874*.
- Lundberg, SM, GG Erion, and SI Lee (2018). Consistent individualized feature attribution for tree ensembles. *arXiv preprint arXiv:1802.03888*.
- Maaten, L van der and G Hinton (2008). Visualizing Data Using t-SNE. *Journal of machine learning research* **9**(Nov), 2579–2605.
- Matejka, J and G Fitzmaurice (2017). Same Stats, Different Graphs: Generating Datasets with Varied Appearance and Identical Statistics through Simulated Annealing. en. In: *Proceedings of the 2017 CHI Conference on Human Factors in Computing Systems - CHI '17*. Denver, Colorado, USA: ACM Press, pp.1290–1294. <http://dl.acm.org/citation.cfm?doid=3025453.3025912> (visited on 12/19/2018).
- Munzner, T (2014). *Visualization analysis and design*. AK Peters/CRC Press.
- Nelson, L, D Cook, and C Cruz-Neira (1998). XGobi vs the C2: Results of an Experiment Comparing Data Visualization in a 3-D Immersive Virtual Reality Environment with a 2-D Workstation Display. en. *Computational Statistics* **14**(1), 39–52.
- O’neil, C (2016). *Weapons of math destruction: How big data increases inequality and threatens democracy*. Crown.
- Ocagne, Md (1885). *Coordonne’s paralle’les et axiales. Me’thode de transformation ge’ome’trique et proce’dé nouveau de calcul graphique de’duits de la considé’ration des coordonne’s paralle’les*. French. Paris: Gauthier-Villars.
- Palan, S and C Schitter (2018). Prolific. A Subject Pool for Online Experiments. *Journal of Behavioral and Experimental Finance* **17**. Publisher: Elsevier, 22–27.

BIBLIOGRAPHY

- Pearson, K (1901). LIII. On lines and planes of closest fit to systems of points in space. *The London, Edinburgh, and Dublin Philosophical Magazine and Journal of Science* **2**(11), 559–572.
- Pedersen, TL and D Robinson (2020). *gganimate: A Grammar of Animated Graphics*. <https://CRAN.R-project.org/package=gganimate>.
- R Core Team (2020). *R: A Language and Environment for Statistical Computing*. Vienna, Austria: R Foundation for Statistical Computing. <https://www.R-project.org/>.
- Ribeiro, MT, S Singh, and C Guestrin (2016). "Why Should I Trust You?": Explaining the Predictions of Any Classifier. *arXiv:1602.04938 [cs, stat]*. arXiv: 1602.04938. (Visited on 08/20/2018).
- Rodrigues, O (1840). Des lois géométriques qui régissent les déplacements d'un système solide dans l'espace: et de la variation des cordonnées provenant de ces déplacements considérés indépendamment des causes qui peuvent les produire. *Journal de Mathématiques Pures et Appliquées* **5**, 380–440.
- Scrucca, L, M Fop, TB Murphy, and AE Raftery (2016). mclust 5: Clustering, Classification and Density Estimation Using Gaussian Finite Mixture Models. *The R journal* **8**(1), 289–317. (Visited on 08/30/2020).
- Sedlmair, M, T Munzner, and M Tory (2013). Empirical Guidance on Scatterplot and Dimension Reduction Technique Choices. *IEEE Transactions on Visualization & Computer Graphics* (12), 2634–2643.
- Shapley, LS (1953). *A value for n-person games*. Princeton University Press.
- Shmueli, G (2010). To explain or to predict? *Statistical science* **25**(3). Publisher: Institute of Mathematical Statistics, 289–310.
- Shrikumar, A, P Greenside, and A Kundaje (2017). Learning important features through propagating activation differences. In: *International Conference on Machine Learning*. PMLR, pp.3145–3153.
- Shrikumar, A, P Greenside, A Shcherbina, and A Kundaje (2016). Not just a black box: Learning important features through propagating activation differences. *arXiv preprint arXiv:1605.01713*.
- Sievert, C (2020). *Interactive Web-Based Data Visualization with R, plotly, and shiny*. Chapman and Hall/CRC. <https://plotly-r.com>.

BIBLIOGRAPHY

- Silva, N da, D Cook, and EK Lee (2021). A Projection Pursuit Forest Algorithm for Supervised Classification. *Journal of Computational and Graphical Statistics*. Publisher: Taylor & Francis, 1–21.
- Simonyan, K, A Vedaldi, and A Zisserman (2014). Deep inside convolutional networks: Visualising image classification models and saliency maps. In: *In Workshop at International Conference on Learning Representations*. Citeseer.
- Spyrison, N and D Cook (2020). spinifex: an R Package for Creating a Manual Tour of Low-dimensional Projections of Multivariate Data. en. *The R Journal* **12**(1), 243. (Visited on 10/16/2020).
- Spyrison, N, B Lee, and L Besançon (2021). "Is IEEE VIS *that* good?" On key factors in the initial assessment of manuscript and venue quality. *OSF preprints*. type: article. (Visited on 08/21/2021).
- Swayne, DF, DT Lang, A Buja, and D Cook (2003). GGobi: evolving from XGobi into an extensible framework for interactive data visualization. *Computational Statistics & Data Analysis. Data Visualization* **43**(4), 423–444. (Visited on 12/19/2018-12-19).
- Tukey, JW (1977). *Exploratory data analysis*. Vol. 32. Pearson.
- Vanni, L, M Ducoffe, C Aguilar, F Precioso, and D Mayaffre (2018). Textual Deconvolution Saliency (TDS): a deep tool box for linguistic analysis. In: *Proceedings of the 56th Annual Meeting of the Association for Computational Linguistics (Volume 1: Long Papers)*, pp.548–557.
- Wagner Filho, J, M Rey, C Freitas, and L Nedel (2018). Immersive Visualization of Abstract Information: An Evaluation on Dimensionally-Reduced Data Scatterplots. In:
- Wang, BT, TJ Hobbs, S Doyle, J Gao, TJ Hou, PM Nadolsky, and FI Olness (2018). Mapping the sensitivity of hadronic experiments to nucleon structure. *Physical Review D* **98**(9), 094030.
- Wickham, H and G Grolemund (2017). *R for Data Science*. O'Reilly Media. <https://r4ds.had.co.nz/index.html>.
- Wickham, H (2016). *ggplot2: Elegant Graphics for Data Analysis*. Springer-Verlag New York. <https://ggplot2.tidyverse.org>.

BIBLIOGRAPHY

- Wickham, H, D Cook, and H Hofmann (2015). Visualizing statistical models: Removing the blindfold: Visualizing Statistical Models. en. *Statistical Analysis and Data Mining: The ASA Data Science Journal* **8**(4), 203–225. (Visited on 03/16/2018).
- Wickham, H, D Cook, H Hofmann, and A Buja (2011). tourr: An R Package for Exploring Multivariate Data with Projections. en. *Journal of Statistical Software* **40**(2). (Visited on 11/23/2018-11-23).
- Xie, Y (2016). *bookdown: Authoring Books and Technical Documents with R Markdown*. Boca Raton, Florida: Chapman and Hall/CRC. <https://github.com/rstudio/bookdown>.
- Xie, Y (2020). *knitr: A General-Purpose Package for Dynamic Report Generation in R*. <https://yihui.org/knitr/>.
- Xie, Y, JJ Allaire, and G Grolemund (2018). *R Markdown: The Definitive Guide*. Boca Raton, Florida: Chapman and Hall/CRC. <https://bookdown.org/yihui/rmarkdown>.
- Yanai, I and M Lercher (2020). A hypothesis is a liability. *Genome Biology* **21**(1), 231. (Visited on 08/24/2021).
- Yang, L (1999). 3D Grand Tour for Multidimensional Data and Clusters. en. In: *Advances in Intelligent Data Analysis*. Ed. by DJ Hand, JN Kok, and MR Berthold. Lecture Notes in Computer Science. Berlin, Heidelberg: Springer, pp.173–184.
- Yang, L (2000). Interactive exploration of very large relational datasets through 3D dynamic projections. en. In: *Proceedings of the sixth ACM SIGKDD international conference on Knowledge discovery and data mining - KDD '00*. Boston, Massachusetts, United States: ACM Press, pp.236–243. <http://portal.acm.org/citation.cfm?doid=347090.347134> (visited on 07/25/2021).